

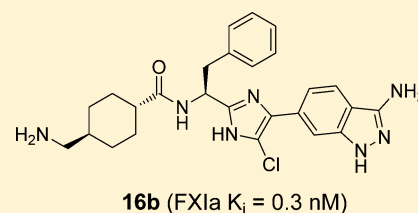
## Phenylimidazoles as Potent and Selective Inhibitors of Coagulation Factor XIa with in Vivo Antithrombotic Activity

Jon J. Hangeland,\* Todd J. Friends, Karen A. Rossi, Joanne M. Smallheer, Cailan Wang, Zhong Sun, James R. Corte, Tianan Fang, Pancras C. Wong, Alan R. Rendina, Frank A. Barbera, Jeffrey M. Bozarth, Joseph M. Luettggen, Carol A. Watson, Ge Zhang, Anzhi Wei, Vidhyashankar Ramamurthy, Paul E. Morin, Gregory S. Bisacchi, Srinath Subramaniam, Piramanayagam Arunachalam, Arvind Mathur, Dietmar A. Seiffert, Ruth R. Wexler, and Mimi L. Quan

Research and Development, Bristol-Myers Squibb, P.O. Box 5400, Princeton, New Jersey 08543, United States

## S Supporting Information

**ABSTRACT:** Novel inhibitors of FXIa containing an (*S*)-2-phenyl-1-(4-phenyl-1*H*-imidazol-2-yl)ethanamine core have been optimized to provide compound **16b**, a potent, reversible inhibitor of FXIa ( $K_i = 0.3$  nM) having in vivo antithrombotic efficacy in the rabbit AV-shunt thrombosis model ( $ID_{50} = 0.6$  mg/kg + 1 mg kg<sup>-1</sup> h<sup>-1</sup>). Initial analog selection was informed by molecular modeling using compounds **11a** and **11h** overlaid onto the X-ray crystal structure of tetrahydroquinoline **3** complexed to FXIa. Further optimization was achieved by specific modifications derived from careful analysis of the X-ray crystal structure of the FXIa/**11h** complex. Compound **16b** was well tolerated and enabled extensive pharmacologic evaluation of the FXIa mechanism up to the  $ID_{90}$  for thrombus inhibition.



## INTRODUCTION

Thromboembolic disorders such as stroke, myocardial infarction, and deep vein thrombosis remain a leading cause of death in developed countries.<sup>1</sup> Normal hemostasis is a tightly regulated process that balances the need for blood to maintain a fluid state under normal physiologic conditions while providing a mechanism for the rapid formation of hemostatic plugs at sites of injury to prevent life threatening loss of blood. The coagulation cascade contains multiple plasma serine protease zymogens organized in a cascade that serves to amplify an initiation event such as blood vessel wall injury, leading to the formation of a hemostatic plug under normal physiologic conditions or the pathophysiologic formation of an interarterial thrombus at the site of a ruptured atherosclerotic plaque.<sup>1a</sup> The cascade can be divided into three interdependent pathways; the extrinsic, intrinsic, and common pathways.<sup>2a–d</sup> Initiation of the extrinsic pathway occurs when injury to the blood vessel wall exposes FVII or its activated form (FVIIa) to the integral membrane protein tissue factor (TF) to form the TF/FVIIa complex. This complex converts factor X and factor IX to their active forms (FXa and FIXa, respectively) via limited proteolysis. Factor Xa in turn catalyzes the conversion of prothrombin to thrombin which produces fibrin from fibrinogen. Thrombin has additional roles in the coagulation cascade. These include (1) activation of factor XIII to its activated form, FXIIIa, which catalyzes the cross-linking of fibrin to form a fibrin clot, (2) amplification of its own generation by activating two other coagulation cofactors, FV and FVIII, (3) activation of blood platelets, (4) activation of thrombin-activatable fibrinolysis inhibitor (TAFI), thereby

inhibiting fibrinolysis, and (5) converting FXI to its active form, FXIa, which is positioned near the head of the intrinsic coagulation pathway. FXIa subsequently catalyzes the production of activated FIX (FIXa), which produces more FXa, thus amplifying the amount of thrombin formed at the site of the growing thrombus. FXIa can be formed independent of thrombin via self-activation and by activated FXII (FXIIa), which is activated by polyanionic surfaces (e.g., collagen platelet polyphosphates released by activated platelets),<sup>2e</sup> by self-activation, or by plasma kallikrein.<sup>2f</sup> Current data indicate that nascent blood clots formed through the extrinsic pathway are unstable and relatively short-lived. Thus, initiation of the intrinsic pathway and formation of FXIa by thrombin or FXIIa is thought to be important for maintaining clot integrity,<sup>3a–3c</sup> especially in tissues with high fibrinolytic activity.<sup>3b</sup>

While FXIa appears to play a key role in stable thrombus formation, it is not required for normal hemostasis. Persons deficient in FXI (hemophilia C) may experience bleeding associated with invasive surgical procedures but rarely spontaneous bleeding.<sup>4</sup> In contrast, deficiencies in FIX, or its cofactor FVIII, are associated with a severe bleeding diathesis (hemophilia B and A, respectively).<sup>5</sup> Preclinical studies have shown that FXI-deficient mice were protected against ferric chloride (FeCl<sub>3</sub>) induced carotid artery thrombosis and venous thrombosis while maintaining normal tail bleeding times as compared to wild-type mice. Similar levels of protection against FeCl<sub>3</sub>-induced thrombus formation provided by heparin or

Received: July 15, 2014

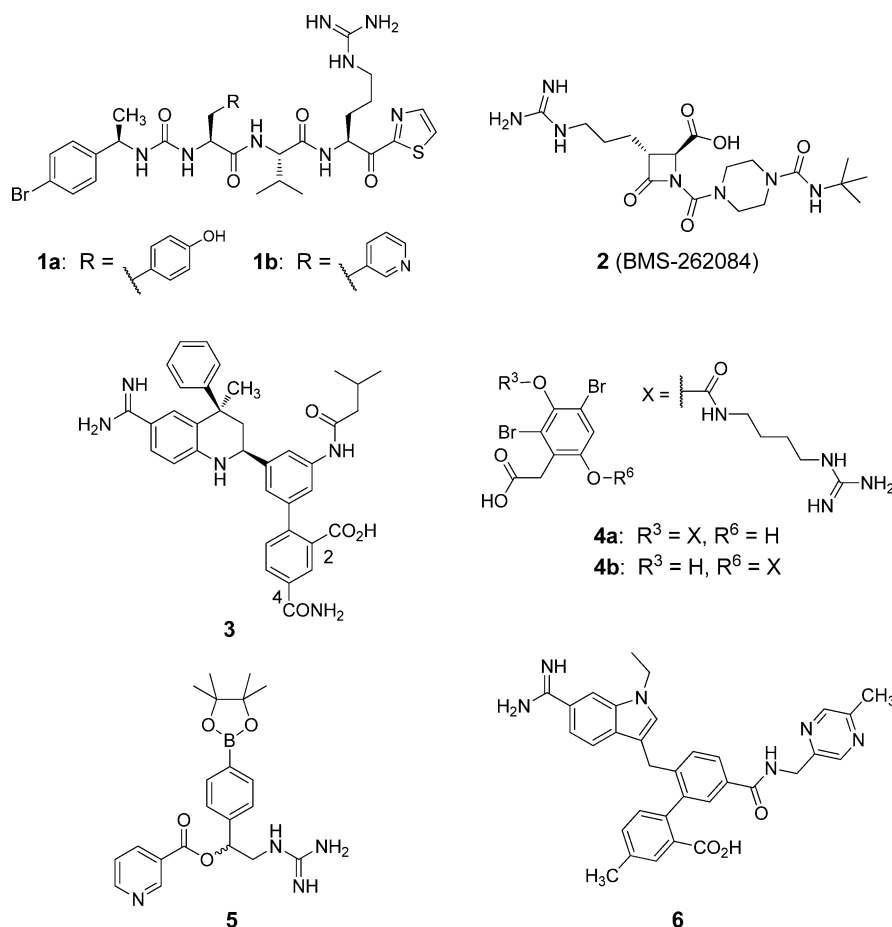


Figure 1. Published active site inhibitors of FXIa.

argatroban, a thrombin inhibitor, resulted in increased bleeding times that were >10-fold longer than that observed in untreated wild type controls.<sup>6</sup> Other studies indicate that elevated FXI levels are associated with venous thrombosis, myocardial infarction among men, increased odds ratio for cerebrovascular events, and coronary artery disease.<sup>7</sup> Conversely, reduced incidence of ischemic stroke, but not myocardial infarction, is observed in subjects with severe FXI deficiency.<sup>8</sup> Taken together, these data support the hypothesis that inhibition of FXIa has the potential to effectively inhibit thrombus formation without significant bleeding liability.<sup>3c–3d</sup>

The first pharmacologic proof of concept studies in rats<sup>9,10a</sup> and rabbits<sup>10b</sup> were conducted with irreversible FXIa small molecule inhibitors using ketothiazoles **1a** and **1b** (FXIa IC<sub>50</sub> = 6 and 12 nM, respectively)<sup>9</sup> and BMS-262084 (**2**) (FXIa IC<sub>50</sub> = 2.8 nM),<sup>10a</sup> a 4-carboxy-2-azetidinone mechanism based inhibitor (Figure 1).<sup>11</sup> These studies demonstrated that inhibition of FXIa significantly reduced thrombus formation in multiple models while causing minimal increase in provoked bleeding times relative to controls. Importantly, the compounds increased in vitro aPTT but not PT, consistent with a FXIa inhibitory mechanism with selectivity over FVIIa, FXa, and thrombin. More recently, tetrahydroquinoline **3**,<sup>12</sup> a small molecule, reversible inhibitor of FXIa ( $K_i$  = 0.2 nM), exhibited a potent dose dependent antithrombotic effect in the rabbit AV-shunt model with no increase in provoked bleeding time relative to untreated controls.<sup>13</sup> Consistent with a selective FXIa mechanism, ex vivo aPTT was prolonged while PT remained unchanged. These studies further support the

hypothesis that selective inhibition of FXIa via a small molecule has the potential to be efficacious with a low bleeding liability.

Additional small molecule FXIa inhibitors have been reported. Two natural products isolated from the sponge *Subera clavata*, clavatadine A (**4a**) and B (**4b**), were shown to be irreversible inhibitors of FXIa (IC<sub>50</sub> = 1.3 and 27 μM, respectively).<sup>14</sup> Arylboronic ester **5** (human FXIa IC<sub>50</sub> = 1.4 μM, 30- and 9-fold selective over FXa and thrombin) represents the most potent inhibitor from an effort to identify arylboronic esters capable of bonding covalently either reversibly or irreversibly to the active site serine.<sup>15</sup> Previous work from our laboratories culminated in the discovery of two series of potent, reversible FXIa inhibitors: the tetrahydroquinoline series (e.g., compound **3**, FXIa  $K_i$  = 0.2 nM)<sup>12</sup> and the indole series (e.g., compound **6**, FXIa  $K_i$  = 0.3 nM).<sup>16</sup> Compound **6** was highly selective against a broad panel of serine proteases including thrombin (27 000-fold), FXa (12 000-fold), FVIIa (>35 500-fold), and plasma kallikrein (PK, 3870-fold) and showed potent in vivo antithrombotic efficacy<sup>16</sup> in the rabbit ECAT model.<sup>18a</sup> All the aforementioned FXIa inhibitors bind to the active or orthosteric site of the enzyme competing with the peptide substrate for binding. Alternatively, binding to the heparin-binding sites (HBS) on FXIa can inhibit the enzyme via an allosteric mechanism through induction of conformational changes that disfavor efficient enzyme catalysis leading to full or partial inhibitors.<sup>17</sup>

In order to provide additional chemotypes to test the FXIa mechanism in preclinical models, we developed a third, novel chemotype built on the phenylimidazole scaffold. We report

Table 1. In Vitro and aPTT Data for Compounds 3, 11a–h, and 11l–s

compd	R <sup>3'</sup>	R <sup>4'</sup>	K <sub>i</sub> (nM) <sup>a</sup>				EC <sub>2X</sub> (μM), <sup>b</sup> aPTT
			FXIa	FVIIa	FXa	PK	
3			0.2	630	340	2	2
11a	H	H	120	>10900	>8180	330	>40
11b	H	CN	230	>10900	>8180	940	NT <sup>d</sup>
11c	H	CO <sub>2</sub> Me	800	>10900	>8180	1924	NT <sup>d</sup>
11d	H	CH <sub>2</sub> CO <sub>2</sub> Et	495	>10900	>8180	1360	NT <sup>d</sup>
11e	CN	H	1120	>10900	>8180	1170	NT <sup>d</sup>
11f	CH <sub>2</sub> CO <sub>2</sub> Et	H	630	>10900	>8180	1470	NT <sup>d</sup>
11g	H	SO <sub>2</sub> NH <sub>2</sub>	1340	>10900	>8180	5540 <sup>c</sup>	NT <sup>d</sup>
11h	H	CONH <sub>2</sub>	30	>10900	>9000	60	>40
11l	H	CO <sub>2</sub> H	590	>10900	>8180	3820	NT <sup>d</sup>
11m	H	CONHMe	350	>10900	>8180	220	NT <sup>d</sup>
11n	H	CON(Me) <sub>2</sub>	2860	>10900	>8180	5270 <sup>c</sup>	NT <sup>d</sup>
11o	H	CH <sub>2</sub> CO <sub>2</sub> H	150	>10900	>8180	765	NT <sup>d</sup>
11p	H	CH <sub>2</sub> CONH <sub>2</sub>	400	>10900	>8180	1310	NT <sup>d</sup>
11q	CONH <sub>2</sub>	H	1100	>10900	>8180	910	NT <sup>d</sup>
11r	CH <sub>2</sub> CO <sub>2</sub> H	H	275	>10900	>8180	920	NT <sup>d</sup>
11s	CH <sub>2</sub> CONH <sub>2</sub>	H	545	>10900	>8180	1902	NT <sup>d</sup>

<sup>a</sup>K<sub>i</sub> values were obtained from purified human enzymes and are averaged from duplicate IC<sub>50</sub> determinations. <sup>b</sup>Activated partial thromboplastin time (aPTT) was measured according to the method described in the Experimental Section. <sup>c</sup>Values reported from a single determination (*n* = 1). <sup>d</sup>NT = not tested.

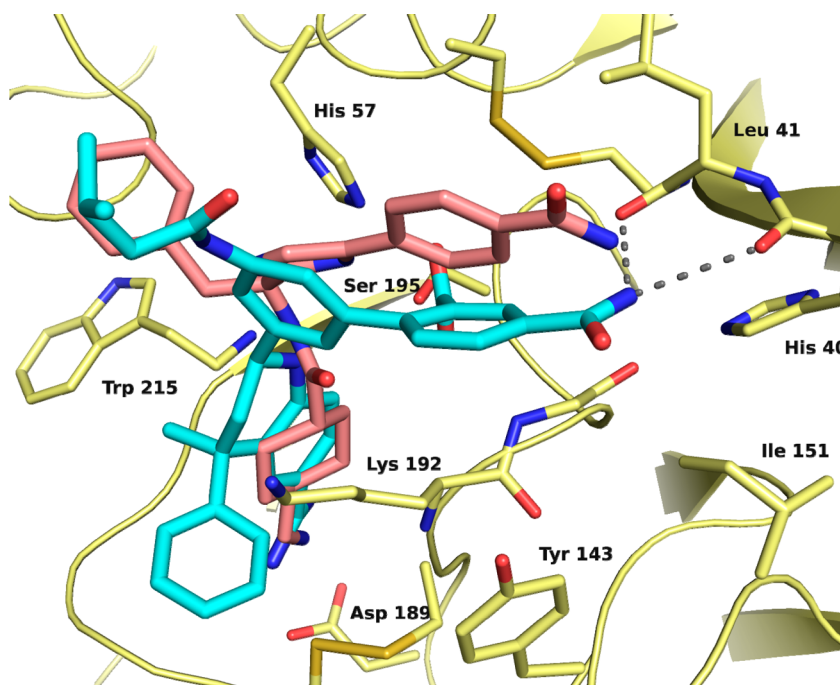


**Figure 2.** Computer model of compound 11h (salmon) overlaid onto the X-ray crystal structure of compound 3/FXIa complex (cyan). Hydrogen bonds between the amide nitrogen located at C-4 of the terminal phenyl ring of the biphenyl contained in compound 3 are represented by a series of gray prolate ellipsoids. Figure was prepared with PyMol (Schrödinger).

herein optimization of the potency for FXIa inhibition of novel, reversible FXIa inhibitors resulting in the identification of *trans*-N-((S)-1-(4-(3-amino-1*H*-indazol-6-yl)-5-chloro-1*H*-imidazol-2-yl)-2-phenylethyl)-4-(aminomethyl)cyclohexanecarboxamide (**16b**, Scheme 2) having potent in vivo antithrombotic activity.

## RESULTS AND DISCUSSION

The first example in the new series, compound 11a (*S*-configuration), was discovered by focused-deck screening against FXIa. It was modestly potent against FXIa (*K<sub>i</sub>* = 120

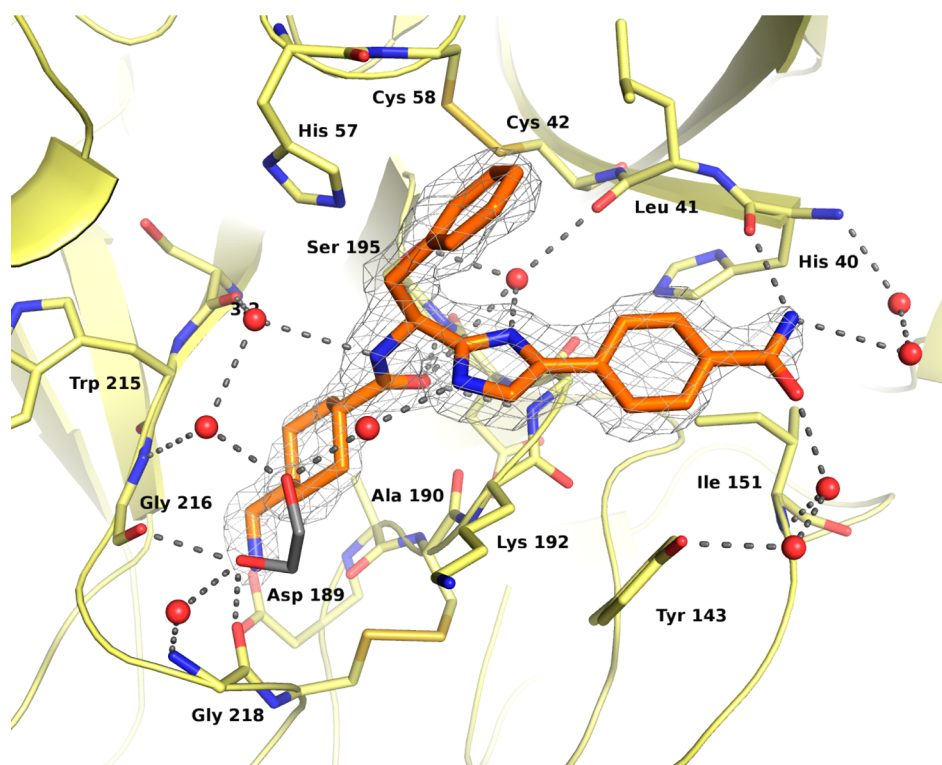


**Figure 3.** X-ray crystal structure of compound **11h** complexed to FXIa. The initial  $F_o - F_c$  electron density contoured at 3 rmsd is shown with the final model. The protein is shown with yellow carbon atoms and secondary structural elements, and **11h** is shown with orange carbon atoms. Nitrogen atoms are shown in blue, oxygen atoms in red, and sulfur atoms in a darker yellow. The red spheres represent crystallographic water molecules. A single crystallographic ethylene glycol molecule is present. Hydrogen bonds are represented by a series of gray prolate ellipsoids. Figure was prepared with PyMol (Schrödinger).

nM) and plasma kallikrein (PK,  $K_i = 330$  nM) and selective against FVIIa ( $K_i > 10\,900$  nM) and FXa ( $K_i > 8180$  nM) and increased aPTT 1.4-fold at a plasma concentration of  $40\ \mu\text{M}$  (Table 1). The enantiomer of **11a** (*R*-configuration) (FXIa  $K_i = 3500$  nM) was 30-fold less potent against FXIa; hence, the SAR was developed using the series with the *S*-configuration. Computer assisted modeling of compound **11a** docked with the X-ray crystal structure of compound **3** complexed to FXIa<sup>12</sup> revealed that the phenylimidazole phenyl ring of **11a** could potentially overlap with the terminal phenyl ring of the biphenyl moiety of compound **3** (model not shown). Furthermore, the structure of the compound **3**/FXIa complex (Figure 2) showed the amide nitrogen located at C-4 of the terminal phenyl ring of the biphenyl moiety to participate in key hydrogen bond contacts with the backbone carbonyls of Leu41 and His40 located in the S2' pocket of FXIa. When this functionality was added to the phenylimidazole phenyl ring of the model of compound **11a** giving compound **11h** ( $R^{4'} = \text{CONH}_2$ ; Figure 2), the hydrogen bond interactions between compound **3** and Leu41 and His40 were closely mimicked. Thus, the modeling exercise provided key design insights that focused the initial set of analogs to include functionalities capable of hydrogen bond interactions within the S2' pocket of the enzyme. Selectivity versus other relevant serine proteases was tracked to see if selectivity for FXIa inhibition was maintained.

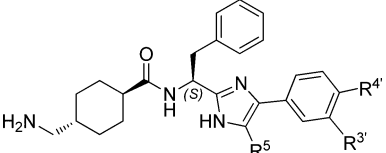
A focused set of functional groups able to form hydrogen bonds appended onto the terminal phenyl ring at C-4' generally provided compounds with weaker potency than **11a** (see compounds **11b–d**, **11g**, and **11l–p**). The single exception from this set was compound **11h**, which was 4-fold more

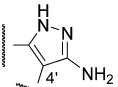
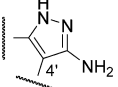
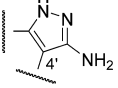
potent against FXIa ( $K_i = 30$  nM), ~2-fold more potent versus PK ( $K_i = 60$  nM), retained excellent selectivity against FVIIa and FXa, and increased aPTT by 1.8-fold at a plasma concentration of  $40\ \mu\text{M}$ . Extending the amide one carbon away from the phenyl ring gave compound **11p**, which was ~10-fold less potent than **11h** against FXIa. Replacing one or both of the primary amide hydrogens of **11h** with a methyl group (compounds **11m** and **11n**, respectively) resulted in an incremental loss of potency against FXIa. A subset of the functional groups tested at C-4' were added to C-3' (compounds **11e**, **11f**, and **11q–s**). All of these compounds were less potent compared to compounds **11a** and **11h**.

The X-ray crystal structure of compound **11h** complexed to FXIa, determined to 1.85 Å resolution, revealed key hydrogen bonds and hydrophobic contacts between the inhibitor and enzyme and an extensive hydrogen bond network between the inhibitor and enzyme formed by crystallographic water molecules and one ethylene glycol molecule (Figure 3). The nitrogen of the primary amide at C-4' of the phenylimidazole moiety formed a hydrogen bond to the backbone carbonyl of His40, located in the S2' pocket, and to the backbone nitrogen of the same residue via two intervening water molecules. The carbonyl formed a hydrogen bond to the backbone nitrogen of Ile151 via one intervening water molecule and to the hydroxyl group of Tyr143 via two intervening water molecules. The phenyl ring formed a hydrophobic contact with side chain of Ile151 and Gly193 within the same pocket. The N-3 nitrogen of the imidazole participated in a hydrogen bond with the backbone carbonyl of Leu41 via an intervening water molecule, whereas N-1 formed a hydrogen bond with a water molecule that was part of a network of three water molecules and one



Table 2. In vitro and aPTT Data for Compounds 11h–k and 16a–c



compd	R <sup>3'</sup>	R <sup>4'</sup>	R <sup>5</sup>	K <sub>i</sub> (nM) <sup>a</sup>				EC <sub>2x</sub> (μM) <sup>b</sup>	
				FXIa	FVIIa	FXa	PK	aPTT	
11h	H	CONH <sub>2</sub>	H	30	>10900	>9000	60	50	
11i	H	CONH <sub>2</sub>	Br	9	>10900	>8180	45	10	
11j	H	CONH <sub>2</sub>	Cl	4	>10900	>9000	20	6	
11k	H	CONH <sub>2</sub>	F	3	>13390	1370	8	2	
16a			H	3	>10,900	>8180	50	2	
16b			Cl	0.3	4220	6390	5	1	(2) <sup>c</sup>
16c			F	0.3	6200	>8180	2	0.5	

<sup>a</sup>K<sub>i</sub> values were obtained from purified human enzymes and are averaged from duplicate IC<sub>50</sub> determinations. <sup>b</sup>Activated partial thromboplastin time (aPTT) was measured according to the method described in the Experimental Section. <sup>c</sup>Rabbit aPTT value.

Table 3. Serine Protease Selectivity and aPTT and PT Data for Compound 16b

K <sub>i</sub> (nM) <sup>a</sup>									EC <sub>2x</sub> (μM) <sup>b</sup>	
FXIa	FXa	FVIIa	FXIIa	FIXa	thrombin	PK	trypsin	chymotrypsin	aPTT	PT
0.3	6390	4220	9218	>34900	>12610	5	23	>20800	1	>40

<sup>a</sup>K<sub>i</sub> values were obtained from purified human enzymes and are averaged from duplicate IC<sub>50</sub> determinations. <sup>b</sup>Activated partial thromboplastin time (aPTT) and prothrombin time (PT) were measured according to the method described in the Experimental Section.

ethylene glycol molecule linking the inhibitor to backbone nitrogens of Gly216 and Gly218. The C-5 methine of the imidazole was located nearby the hydrophobic side chain of Lys192. The benzyl side chain phenyl ring participated in a hydrophobic edge-on contact with the disulfide bridge formed between Cys42 and Cys58 in the S1' pocket. The NH of the P1 group amide linker formed a hydrogen bond to Ser214 via a single intervening water molecule and Gly216 via two intervening water molecules. The carbonyl oxygen of the amide linker was positioned over the oxyanion hole formed by Ser195, Asp194, and Gly193. The tranexamic acid moiety was located in the S1 pocket where the primary amine formed a salt bridge with the carboxylate of Asp189 and the backbone carbonyl of Gly218. Thus, compound 11h formed a hydrogen bond network with the same two S2' pocket protein backbone carbonyls as compound 3 (His40 and Leu41), albeit in a different manner owing to the phenylimidazole phenyl ring of 11h penetrating deeper into the S2' binding pocket compared to the terminal phenyl ring of the biphenyl moiety of compound 3.

Closer examination of hydrogen bond opportunities available in the S2' pocket revealed the backbone carbonyl of His40, the C-4' amide of the inhibitor, and the hydroxyl group of Tyr143, located opposite the backbone carbonyl in the S2' pocket, to be coplanar. We hypothesized that fusing the C-4' amide onto the phenyl ring to form a five- or six-membered ring containing a heteroatom able to form a hydrogen bond to the hydroxyl group of Tyr143 might improve potency. This hypothesis was tested by modifying the terminal phenyl ring to give aminimidazole 16a (Table 2) having a FXIa K<sub>i</sub> = 3 nM, which was 10-fold more potent than 11h against FXIa, ~10-fold selective versus PK (K<sub>i</sub> = 50 nM), and showed potent aPTT activity (EC<sub>2x</sub> = 2 μM). Thus, two novel modifications to the original compound in this series (11a) provided a 40-fold overall improvement to FXIa potency.

The effect of substitution at the C-5 position of the imidazole was first investigated by adding bromine to compound 11h giving compound 11i (Table 2). A 3-fold improvement in potency was realized (FXIa K<sub>i</sub> = 9 nM), and the aPTT assay showed it to have good in vitro anticoagulant activity (EC<sub>2x</sub> =

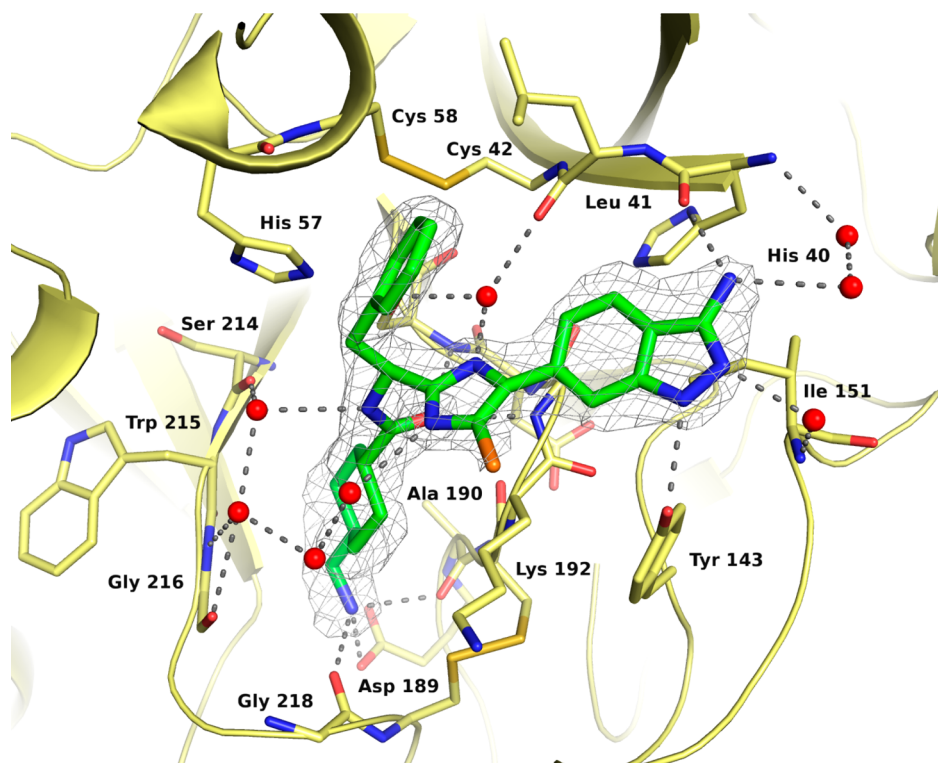


**Figure 4.** X-ray crystal structure of compound **16b** complexed to FXIa. The initial  $F_o - F_c$  electron density contoured at 4 rmsd is shown with the final model. The protein is shown with yellow carbon atoms and secondary structural elements, and **16b** is shown with green carbon atoms. Nitrogen atoms are shown in blue, oxygen atoms in red, sulfur atoms in a darker yellow, and the chlorine atom in orange. The red spheres represent crystallographic water molecules. Hydrogen bonds are represented by a series of gray prolate ellipsoids. Figure was prepared with PyMol (Schrödinger).

10  $\mu\text{M}$ ). Substituting the bromine with chlorine gave compound **11j** (FXIa  $K_i = 4$  nM, aPTT  $\text{EC}_{2x} = 6$   $\mu\text{M}$ ), which showed a similar improvement in potency compared to compound **11h**. The C-5 fluoride (**11k**) was as potent against FXIa as compound **11j** but was less selective against FXa ( $K_i = 1370$  nM) and PK ( $K_i = 8$  nM). Combining all the modifications that improved potency against FXIa into a single molecule gave compound **16b** having subnanomolar potency against FXIa ( $K_i = 0.3$  nM), 17-fold selectivity versus PK, potent in vitro aPTT activity ( $\text{EC}_{2x} = 1$   $\mu\text{M}$ ), and >1000-fold selectivity versus other relevant proteases (see Table 3 for a compilation of data for **16b**). The enantiomer of **16b** (R-configuration) (FXIa  $K_i = 21$  nM) was 70-fold less potent. The C-5 fluoride analog of **16b**, compound **16c**, was equally potent against FXIa ( $K_i = 0.3$  nM) and equally selective against FVIIa, FXa, and PK.

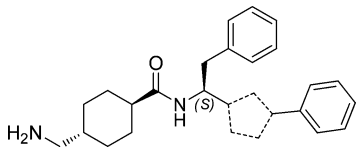
X-ray crystal data (2.09 Å resolution) showed the binding modes of compounds **16b** and **11h** to be virtually identical (Figure 4). The exocyclic nitrogen of the aminoindazole moiety formed a hydrogen bond to the backbone carbonyl of His40 and, via two intervening water molecules, to the backbone nitrogen of the same residue (cf. the amine of the primary amide of **11h**). The N-1 nitrogen of the indazole ring was within hydrogen bonding distance to the hydroxy group of Tyr143 as designed. The N-2 nitrogen participated in a hydrogen bond with the backbone nitrogen of Ile151 via an intervening water molecule (cf. the carbonyl of the primary amide of **11h**). In addition, the C-5 chlorine formed a hydrophobic contact to the aliphatic portion the Lys192 side chain. Combined, the modifications made to compound **11a**, guided by key computer modeling exercises, resulted in a 400-

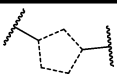
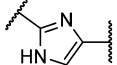
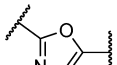
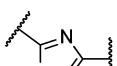
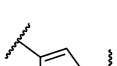
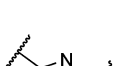
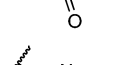
fold improvement in potency for FXIa. In addition, compound **16b** maintained excellent selectivity against a panel of serine proteases found in the coagulation pathway and had good selectivity against PK.

Other five-membered ring heterocycle replacements of the imidazole were surveyed in parallel with the SAR development of the phenylimidazole series (Table 4). 5-Phenyloxazole **20** (FXIa  $K_i = 1440$  nM) was 12-fold less potent for FXIa compared to compound **11a** (FXIa  $K_i = 120$  nM) with good selectivity over FVIIa and FXa and moderate selectivity over PK (2-fold). Replacing the C-5 methine of compound **11a** with nitrogen to give 3-phenyltriazole **22** resulted in an 8-fold loss in potency while maintaining a similar selectivity profile versus FVIIa, FXa, and PK. Interchanging the C-5 methine with the N-3 nitrogen of the imidazole provided 3-phenylpyrazole **27** (FXIa  $K_i = 6940$  nM) resulting in significant loss of potency for FXIa (~60-fold). The 5-oxo-1-phenyltriazole **30** was ~25-fold less potent than imidazole **11a** but retained good selectivity over FVIIa and FXa. The 2-phenylimidazole regioisomer of **11a**, compound **33** (FXIa  $K_i = 1640$  nM), was similar in potency and selectivity to oxazole **20**. In conclusion, the 5-phenylimidazole regioisomer contained in **11a** remained the most potent five-membered ring heterocycle analog among the small set surveyed.

Compound **16b** exhibited reversible enzyme inhibition kinetics at 37 °C (FXIa  $K_i = 0.82$  nM, on rate =  $3.0 \mu\text{M}^{-1} \text{s}^{-1}$ ,  $t_{1/2}$  off = 4.6 min), with similar potency for rabbit coagulation factor orthologs (Table 5). Pharmacokinetic profiling of compound **16b** in rabbits by iv administration at 0.5 mg/kg showed the compound to be relatively rapidly cleared and to have a relatively low volume of distribution

Table 4. In Vitro Data for Compounds 11a, 20, 22, 27, 30, 33



compd		$K_i$ (nM) <sup>a,b</sup>	
		FXIa	PK
11a		120	330
20		1440	3440
22		980	2217
27		6940	5023
30		3074	4820
33		1640	4500

<sup>a</sup> $K_i$  values were obtained from purified human enzymes and are averaged from duplicate  $IC_{50}$  determinations. <sup>b</sup> $K_i > 10\,900$  nM and  $K_i > 8180$  nM for FVIIa and FXa, respectively.

(Table 6). The compound was 85% protein bound in rabbit serum. Compound 16b was not orally bioavailable; however, the bis-HCl salt had ample solubility (946  $\mu\text{g/mL}$  in 100 mM phosphate buffer, pH 7.4; amorphous solid) for iv administration. When tested using the rabbit AV-shunt model<sup>18a</sup> at three doses administered as a single loading dose followed by continuous iv infusion to maintain steady state blood levels of drug, the bis-HCl salt of compound 16b showed potent dose dependent in vivo antithrombotic activity relative to untreated controls with a calculated  $ID_{50} = 0.6 \text{ mg/kg} + 1 \text{ mg kg}^{-1} \text{ h}^{-1}$  (Figure 5). Inhibition of plasma kallikrein (PK) may contribute to the antithrombotic effect of compound 16b, since the selectivity of compound 16b for rabbit FXIa versus rabbit PK

inhibition is modest (35-fold) and PK KO mice have been shown to be resistant to thrombus formation in mouse venous and arterial  $\text{FeCl}_3$ -induced thrombosis models.<sup>19</sup>

## CHEMISTRY

Phenylimidazoles 9a–g were synthesized using a three-step sequence<sup>20</sup> (Scheme 1). The cesium salt of (L)-N-Boc-phenylalanine (7), formed using cesium carbonate in ethanol/water (1:1), was combined with the appropriately substituted bromoacetophenones 8a–g. The resulting  $\beta$ -keto esters were condensed with ammonium acetate (refluxing xylenes, Dean–Stark trap) to give the phenylimidazoles 9a–g. Yields for this three-step sequence ranged between 40% and 60%. Removal of the Boc group with 10% trifluoroacetic acid (v/v) in methylene chloride at room temperature was followed by amide bond formation (BOP reagent or EDC/HOBT) with N-Boc-tranexamic acid to give intermediates 10a–g. Nitriles 10b and 10e were hydrolyzed to the primary amides 10h and 10q, respectively, using 30% hydrogen peroxide and potassium carbonate in DMSO. Addition of magnesium oxide to the reaction with 10h helped to accelerate an otherwise sluggish hydrolysis. Addition of bromine to C-5 of the imidazole ring was accomplished by reacting intermediate 10h with bromine in methylene chloride at room temperature to give 10i. Synthesis of the C-5 chloro analog 10j began with hydrolysis of nitrile 9b using potassium carbonate, hydrogen peroxide, and magnesium oxide followed by chlorination of the C-5 carbon of the imidazole with N-chlorosuccinimide in refluxing acetonitrile. Removal of the Boc group with TFA and addition of N-Boc-tranexamic acid using BOP/pyridine gave 10j. The C-5 fluoro analog 10k was obtained by reaction of 10h with SelectFluor in DMF/ $\text{H}_2\text{O}$  (10:1). Esters 10c, 10d, and 10f were hydrolyzed to the corresponding acids 10l, 10o, and 10r using methanolic sodium hydroxide at room temperature. Again, use of magnesium oxide accelerated the otherwise slow hydrolysis of ester 10c. Carboxylic acid 10l was converted to monomethylamide 10m or dimethylamide 10n using methylamine or dimethylamine, respectively (EDC/HOBT). The primary phenylacetamides 10p and 10s were synthesized from the corresponding phenylacetic acids 10o and 10r using EDC/HOAt and N-methylmorpholine followed by concentrated aqueous ammonia. The Boc group on the tranexamic acid moiety for intermediates 10a–s was removed using 10% trifluoroacetic acid (v/v) in methylene chloride at room temperature to provide compounds 11a–s as bis-trifluoroacetic acid salts.

Aminoindazoles 16a–c were accessed starting from commercially available 4-bromo-3-fluorobenzoic acid (12), which was treated with zinc(II) cyanide and tetrakis-(triphenylphosphine)palladium(0) in dimethylformamide at 90 °C to give 4-cyano-3-fluorobenzoic acid (Scheme 2). The carboxylic acid was converted to  $\alpha$ -bromoketone 13 by a three-step, one-pot transformation: (1) formation of the acid chloride

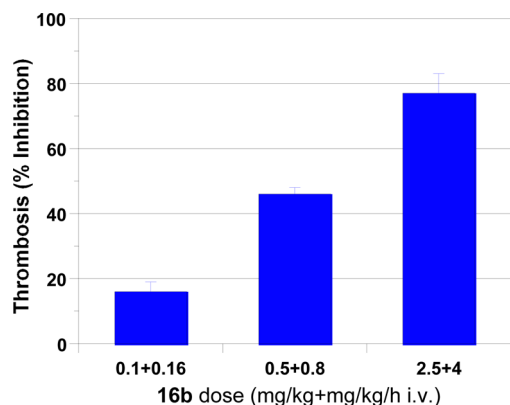
Table 5. Comparison of Human and Rabbit Selectivity Profile and in Vitro aPTT for Compound 16b

species	$K_i$ (nM) <sup>a</sup>					$EC_{2x}$ ( $\mu\text{M}$ ), <sup>b</sup> aPTT
	FXIa	FXa	thrombin	FVIIa	PK	
human	0.3 (0.8) <sup>c</sup>	6390	>12610	4220	5	1
rabbit	0.6 (1.2) <sup>c</sup>	>10000	>20000	10000 <sup>c</sup>	21	2

<sup>a</sup> $K_i$  values were obtained from purified human enzymes and are averaged from duplicate  $IC_{50}$  determinations. <sup>b</sup>Activated partial prothrombin time (aPTT) was measured according to the method described in the Experimental Section. <sup>c</sup>Values were determined at 37 °C.

Table 6. Rabbit Pharmacokinetic and Protein Binding Data for Compound 16b

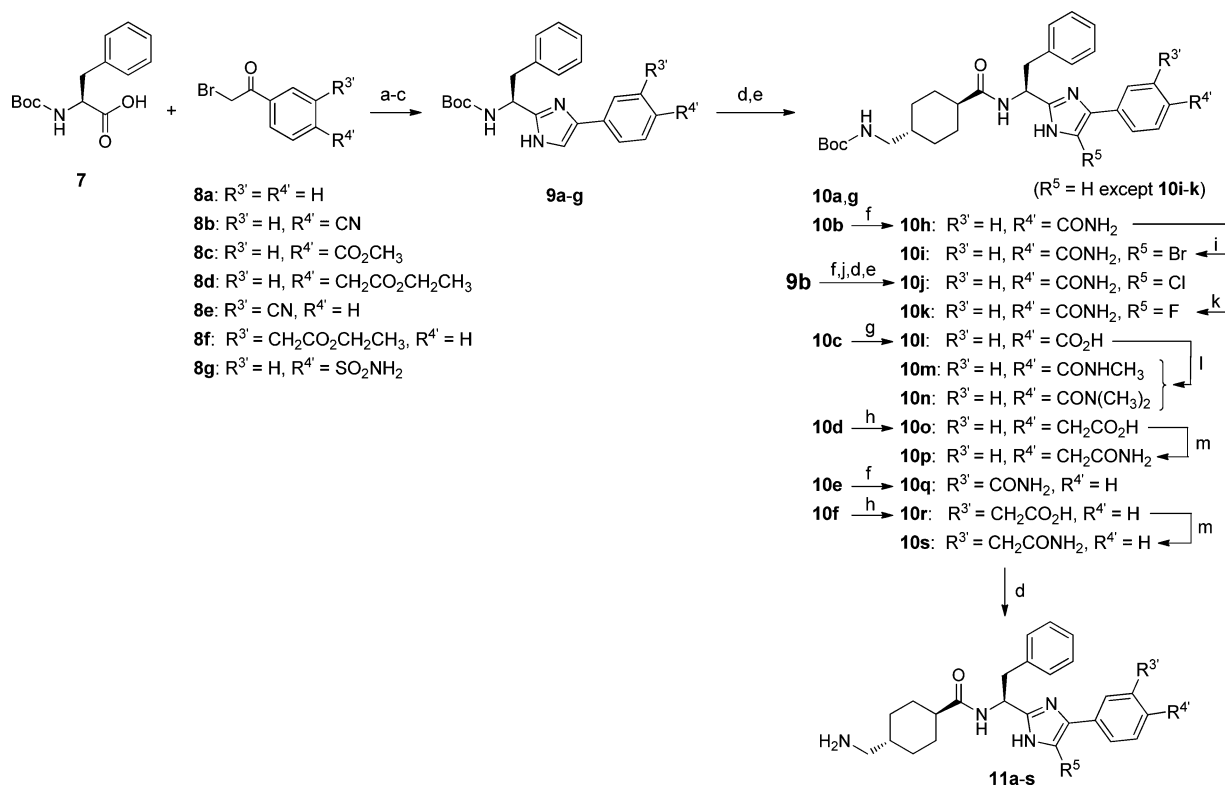
dose (mg/kg)	C <sub>max</sub> (nM)	CL (L h <sup>-1</sup> kg <sup>-1</sup> )	V <sub>ss</sub> (L/kg)	t <sub>1/2</sub> (h)	MRT (h)	protein binding <sup>a</sup> (%)
0.5	2472 ± 456	1.2 ± 0.1	0.7 ± 0.1	1.0 ± 0.3	0.6 ± 0.1	85

<sup>a</sup>Determined using rabbit plasma.

**Figure 5.** Rabbit AV-shunt data. Compound 16b was given as a single loading dose followed by continuous iv infusion at three doses: 0.1 mg/kg + 0.16 mg kg<sup>-1</sup> h<sup>-1</sup>, 0.5 mg/kg + 0.8 mg kg<sup>-1</sup> h<sup>-1</sup>, 2.5 mg/kg + 4 mg kg<sup>-1</sup> h<sup>-1</sup>. Thrombi formed were removed from the shunt and weighed. % inhibition values are relative to thrombus formation prior to drug treatment. ID<sub>50</sub> = 0.6 mg/kg + 1 mg kg<sup>-1</sup> h<sup>-1</sup>.

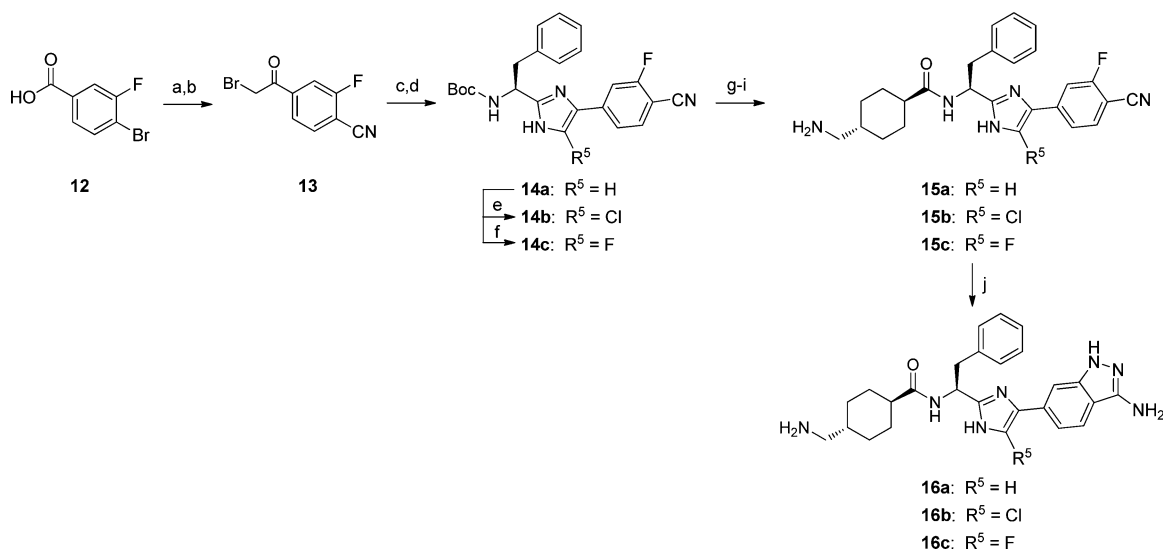
using oxalyl chloride in methylene chloride, (2) conversion of the acid chloride to the methyl ketone with trimethylsilyldiazomethane in acetonitrile (1 h at -15 °C, then reflux for 1 h), and (3) bromination of the methyl ketone (33% hydrobromic acid in acetic acid, -15 °C). The sequence carrying bromoketone 13 forward to imidazole 14a (R<sup>5</sup> = H) was the same as described for compounds 10a–g. Refluxing 14a with *N*-chlorosuccinimide in acetonitrile gave chloroimidazole 14b. SelectFluor in DMF/H<sub>2</sub>O (10:1) gave fluoroimidazole 14c from 14a. Imidazoles 14a–c were carried forward to 15a–c, respectively, using the reaction sequence described for converting compounds 9a–g to 11a–g. Compounds 15a–c were treated with hydrazine hydrate in *n*-butanol at 120 °C for 1 h to give the corresponding aminoimidazoles 16a–c, which were isolated as bis-trifluoroacetic acid salts. Alternatively, the final two steps in the sequence (Scheme 2, steps i and j) could be reversed. Formation of the bis-HCl salt of 16b used in the rabbit AV-shunt model was obtained using reverse phase HPLC with a mobile phase containing HCl.

Synthesis of 5-phenyloxazole 20 (Scheme 3) began with amide coupling between (*S*)-2-(1,3-dioxoisindolin-2-yl)-3-phenylpropanoic acid (17) and 2-amino-1-phenylethanone

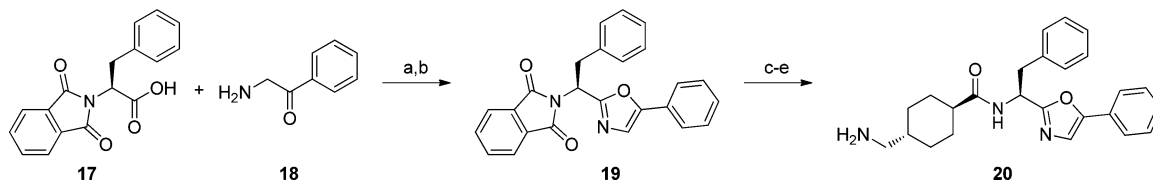
Scheme 1. Synthesis of Phenylimidazoles 11a–s<sup>a</sup>

<sup>a</sup>(a) 7, Cs<sub>2</sub>CO<sub>3</sub>, EtOH/H<sub>2</sub>O (1:1), rt, 1 h; (b) Cs salt from (a), 8a–g, DMF, rt, 1 h; (c) NH<sub>4</sub>OAc, xylenes, reflux (Dean–Stark), 3 h; (d) 10–30% (v/v) TFA, CH<sub>2</sub>Cl<sub>2</sub>, rt; (e) *N*-Boc-tranexamic acid, BOP, pyridine, DMF, rt, 16 h or EDC, HOBt, *N*-methylmorpholine, DMF, rt, 16 h; (f) K<sub>2</sub>CO<sub>3</sub>, 30% aq H<sub>2</sub>O<sub>2</sub>, MgO, DMSO, rt, 4 h; (g) NaOH, MgO, CH<sub>3</sub>OH/EtOAc (5:1), rt, 5 h; (h) NaOH, MeOH, rt, 16 h; (i) Br<sub>2</sub>, CHCl<sub>3</sub>, rt, 16 h; (j) NCS, ACN, reflux, 7 h; (k) Selectfluor, DMF/H<sub>2</sub>O (10:1), rt, 2 h; (l) methylamine (10m) or dimethylamine (10n), HOBt, EDC, *N*-methylmorpholine, DMF, rt, 16 h; (m) conc NH<sub>4</sub>OH, HOAt, EDC, *N*-methylmorpholine, DMF, rt, 16 h.

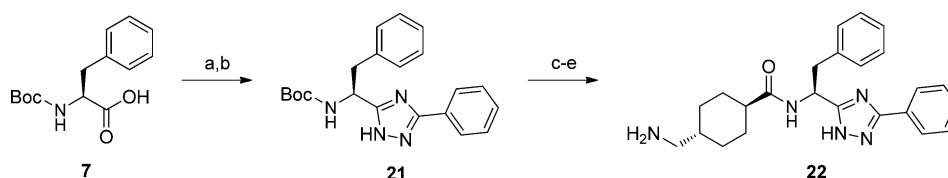


Scheme 2. Synthesis of Aminoindazole Analogs 16a–c<sup>a</sup>

<sup>a</sup>(a)  $\text{Zn}(\text{CN})_2$ ,  $\text{Pd}(\text{PPh}_3)_4$ , DMF, 90 °C, 3 h; (b) (i) oxalyl chloride,  $\text{CH}_2\text{Cl}_2$ , rt, 1 h, then reflux, 1 h, (ii)  $\text{TMSCH}_2\text{N}_2$ , ACN, –15 °C, 1 h, (iii) HBr (33% by mass) in HOAc, –15 °C, 20 min (39% over two steps); (c) 7,  $\text{Cs}_2\text{CO}_3$ , DMF, 15 °C, 1 h (61%); (d)  $\text{NH}_4\text{OAc}$ , xylenes, reflux (Dean–Stark), 2.5 h (41%); (e) NCS, ACN, reflux, 7 h (99%); (f) Selectfluor, DMF/ $\text{H}_2\text{O}$  (10:1), rt, 2 h (27%); (g) 20% TFA (v/v),  $\text{CH}_2\text{Cl}_2$ , rt, 30 min; (h) *N*-Boc-tranexamic acid, BOP, TEA, THF, 75 °C, 15 min; (i) 20% TFA (v/v),  $\text{CH}_2\text{Cl}_2$ , rt, 30 min (>67% for three steps for 15b); (j)  $\text{NH}_2\text{NH}_2 \cdot \text{H}_2\text{O}$ , *n*-BuOH, 120 °C, 1 h (54% for 16b).

Scheme 3. Synthesis of *trans*-4-(Aminomethyl)-*N*-((*S*)-2-phenyl-1-(5-phenyloxazol-2-yl)ethyl)cyclohexanecarboxamide (20)<sup>a</sup>

<sup>a</sup>(a) BOP, anhyd pyridine, rt, 16 h (100%); (b)  $\text{POCl}_3$ , DMF, 90 °C, 30 min (41%); (c) hydrazine, EtOH, reflux, 2 h (90%); (d) *N*-Boc-tranexamic acid, HOAt, EDC, *N*-methylmorpholine, DMF, rt, 1 h; (e) 10% (v/v) TFA,  $\text{CH}_2\text{Cl}_2$ , rt, 16 h (26% over two steps).

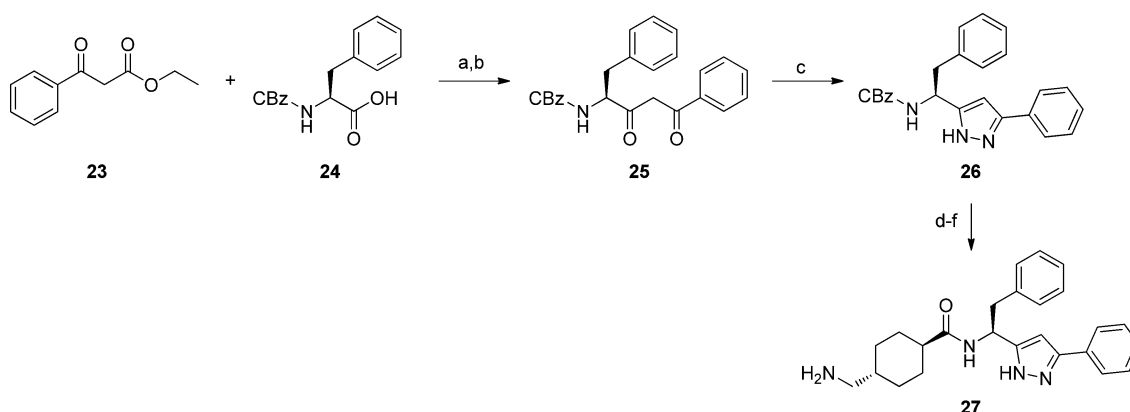
Scheme 4. Synthesis of *trans*-4-(Aminomethyl)-*N*-((*S*)-2-phenyl-1-(3-phenyl-1*H*-1,2,4-triazol-5-yl)ethyl)cyclohexanecarboxamide (22)<sup>a</sup>

<sup>a</sup>(a) Hydrazine, BOP-Cl, anhydrous pyridine, rt, 16 h (100%); (b) ethyl benzimidate-HCl,  $\text{Et}_3\text{N}$ , ACN, reflux, 24 h (42%); (c) 10% (v/v) TFA,  $\text{CH}_2\text{Cl}_2$ , rt, 16 h; (d) *N*-Boc-tranexamic acid, BOP-Cl, anhydrous pyridine, rt, 12 h; (e) 30% (v/v) TFA,  $\text{CH}_2\text{Cl}_2$ , rt, 3 h (28% over three steps).

(18; Bop/pyridine), followed by dehydration of the intermediate diketoamide with  $\text{POCl}_3$  in DMF to give (*S*)-2-(2-phenyl-1-(5-phenyloxazol-2-yl)ethyl)isoindoline-1,3-dione (19). Removal of the phthalimide group with hydrazine in refluxing EtOH was followed by acylation of the free amine with the tranexamic side chain as previously described. The four-step synthesis of 3-phenyltriazole 22 (Scheme 4) began with coupling hydrazine and *N*-Boc-L-phenylalanine 7 using BOP and anhydrous pyridine. The intermediate acyl hydrazide was condensed with ethyl benzimidate hydrochloride in refluxing acetonitrile and TEA to give triazole 21. Removal of the Boc group with TFA and subsequent conversion of the free amine to compound 22 were carried out as before. Synthesis of 3-phenylpyrazine 27 (Scheme 5) began with hydrolysis of ethyl

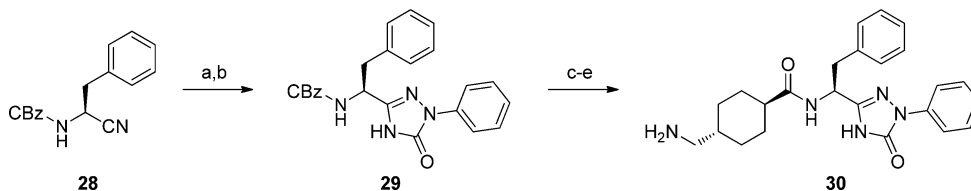
3-oxo-3-phenylpropanoate (23) to give 3-oxo-3-phenylpropanoic acid, followed by formation of magnesium 3-oxo-3-phenylpropanoate using magnesium ethoxide in methanol. The salt was combined with 1,1'-carbonyldiimidazole activated *N*-CBz-L-phenylalanine (24), which resulted in the decarboxylative addition of acetophenone enolate to the mixed anhydride of 24 to give (*S*)-benzyl (3,5-dioxo-1,5-diphenylpentan-2-yl)carbamate (25). The diketone 25 was then condensed with hydrazine in EtOH to give pyrazine 26. Hydrogenation with 10% palladium on carbon followed by installation of the tranexamic side chain provided 3-phenylpyrazine 27. (*S*)-Benzyl (1-cyano-2-phenylethyl)carbamate 28 was converted to the oxotriazine 29 by a three-step process (Scheme 6). First, the methyl imidate of compound 28 was

**Scheme 5. Synthesis of *trans*-4-(Aminomethyl)-*N*-((*S*)-2-phenyl-1-(3-phenyl-1*H*-pyrazol-5-yl)ethyl)cyclohexanecarboxamide (27)<sup>a</sup>**



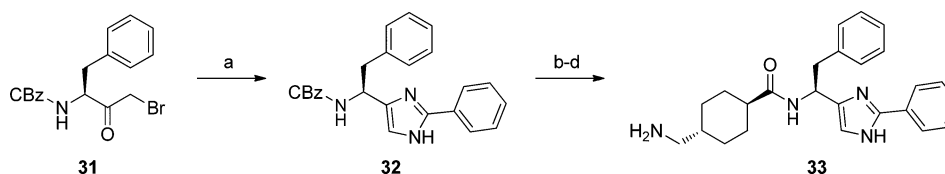
<sup>a</sup>(a) (i) **23**, 1 N NaOH/EtOH (1:1), rt, 72 h; (ii) Mg(OEt)<sub>2</sub>, MeOH, 4 h; (b) (i) **24**, CDI, DMF, 2 h, rt; (ii) intermediate from (a), DMF, rt, 24 h (13%); (c) anhydrous hydrazine, EtOH, 60 °C, 3 h (100%); (d) 10% Pd/C, MeOH, 1 atm H<sub>2</sub>, 4 h (57%); (e) *N*-Boc-tranexamic acid, BOP-Cl, anhydrous pyridine, rt, 12 h; (f) 30% (v/v) TFA, CH<sub>2</sub>Cl<sub>2</sub>, rt, 3 h (46% over two steps).

**Scheme 6. Synthesis of *trans*-4-(Aminomethyl)-*N*-((*S*)-1-(5-oxo-1-phenyl-4,5-dihydro-1*H*-1,2,4-triazol-3-yl)-2-phenylethyl)cyclohexanecarboxamide (30)<sup>a</sup>**



<sup>a</sup>(a) (i) NaOCH<sub>3</sub>, MeOH, 30 °C, 3 h, (ii) HOAc, phenylhydrazine, rt, 18 h (28%); (b) carbonyl diimidazole, THF, reflux, 48 h (66%); (c) 10% Pd/C, MeOH, 1 atm H<sub>2</sub>, 4 h (57%); (d) *N*-Boc-tranexamic acid, BOP-Cl, anhydrous pyridine, rt, 12 h; (e) 30% (v/v) TFA, CH<sub>2</sub>Cl<sub>2</sub>, rt, 3 h (46% over two steps).

**Scheme 7. Synthesis of *trans*-4-(Aminomethyl)-*N*-((*S*)-2-phenyl-1-(2-phenyl-1*H*-imidazol-4-yl)ethyl)cyclohexanecarboxamide 33<sup>a</sup>**



<sup>a</sup>(a) (i) sodium formate, EtOH, reflux, 14 h, (ii) add benzamidine, NaHCO<sub>3</sub>, reflux, 24 h (8%); (b) 10% Pd/C, MeOH, 1 atm H<sub>2</sub>, 4 h (57%); (c) *N*-Boc-tranexamic acid, BOP-Cl, anhydrous pyridine, rt, 12 h; (d) 30% (v/v) TFA, CH<sub>2</sub>Cl<sub>2</sub>, rt, 3 h (46% over two steps).

formed using sodium methoxide. Next, the imidate was condensed with phenylhydrazine to give an iminohydrazide. Third, the iminohydrazide was combined with carbonyl diimidazole in refluxing THF to give the oxotriazole **29**. Synthesis of 5-oxo-1-phenyltriazine **30** from compound **29** was carried out as previously described. Synthesis of 2-phenyl-imidazole **33** (Scheme 7) began by combining bromoketone **31** with sodium formate in refluxing EtOH, followed by addition of benzamidine and sodium bicarbonate to give the imidazole **32**. Removal of the CBz group by hydrogenation as described was followed by acylation with *N*-Boc-tranexamic acid, and subsequent removal of the Boc group with TFA completed the synthesis of 2-phenylimidazole **33**.

## CONCLUSIONS

Optimization of compound **11a** for FXIa potency and selectivity over other relevant serine proteases resulted in the

identification of compound **16b**, a subnanomolar, reversible inhibitor of FXIa. Compound **16b** showed potent dose dependent antithrombotic activity in the rabbit AV-shunt model. It was used extensively in preclinical rabbit efficacy models (AV-shunt,<sup>18a</sup> ECAT,<sup>18b</sup> cuticle bleeding<sup>18c–18d</sup>) to benchmark in vivo efficacy (antithrombotic effect) and safety (bleeding) parameters for this mechanism of action. Compound **16b** was well tolerated in these models and enabled the studies to be conducted up to the ID<sub>90</sub> for thrombus inhibition. A full description of the pharmacology of **16b** and studies identifying orally bioavailable analogs will be published separately.

## EXPERIMENTAL SECTION

All reactions were run under an atmosphere of dry nitrogen or argon unless otherwise noted. Solvents and reagents were obtained from commercial vendors in the appropriate grade and used without further

purification unless otherwise indicated. NMR spectra were obtained on Joel ECP500 (500 MHz) or ECP400 (400 MHz) NMR spectrometers with chemical shift in ppm downfield from TMS as an internal reference standard.  $^1\text{H}$  assignment abbreviations are the following: singlet (s), doublet (d), triplet (t), quartet (q), pentet (p), broad singlet (bs), doublet of doublets (dd), doublet of triplets (dt), and multiplet (m). Flash chromatography was done using Teledyne-ISCO automated flash chromatography instruments. Reverse phase analytical HPLC was performed on Shimadzu LC10AS systems and reverse phase analytical HPLC/MS on Shimadzu LC10AS systems coupled with Waters ZMD mass spectrometers using MeOH/H<sub>2</sub>O containing 0.01% TFA or 10 mM NH<sub>4</sub>OAc as the mobile phase. HPLC purification was performed using a Shimadzu preparative HPLC system composed of a SPD-20A prominence detector, two LC-8A pumps, a SCL-10 vp controller, and a FRC-10 fraction collector using C18 reverse phase columns with MeOH/H<sub>2</sub>O containing 0.05% TFA as the mobile phase. HPLC purity was determined on a Shimadzu LC10AT system equipped with Sunfire C18 and Xbridge phenyl reverse phase columns (3.0 mm × 150 mm) operating at a flow rate of 0.5 mL/min with a mobile phase consisting of H<sub>2</sub>O/acetonitrile containing 0.05% TFA and detector wavelengths set to 220 and 254 nm. All final compounds were found to be >95% pure by HPLC analysis unless otherwise noted.

**Enzyme Affinity Assays.** Factors IXa, Xa, and XIa were purchased from Haematologic Technologies. Factor XIIa was purchased from American Diagnostica. Plasma kallikrein and  $\alpha$ -thrombin were purchased from Enzyme Research Laboratories. Trypsin and chymotrypsin were purchased from Sigma-Aldrich. Recombinant factor VIIa was purchased from Novo Nordisk. Recombinant soluble tissue factor residues 1–219 was produced at Bristol-Myers Squibb.

Factor XIa, factor XIIa, and chymotrypsin assays were conducted in 50 mM HEPES, pH 7.4, 145 mM sodium chloride, 5 mM potassium chloride, and 0.1% PEG 8000. Factor Xa, thrombin, trypsin, and plasma kallikrein assays were conducted in 100 mM sodium phosphate, pH 7.5, 200 mM sodium chloride, and 0.5% PEG 8000. Factor VIIa assays were conducted in 50 mM HEPES, pH 7.4, 150 mM sodium chloride, 5 mM calcium chloride, and 0.1% PEG 8000. Factor IXa assays were conducted in 50 mM Tris, pH 7.4, 100 mM sodium chloride, 5 mM calcium chloride, 0.5% PEG 8000, and 2% DMSO. The peptide substrates were the following: pyro-Glu-Pro-Arg-pNA(*p*-nitroaniline) (Diapharma) for factor XIa and thrombin; N-benzoyl-Ile-Glu-(OH, OMe)-Gly-Arg-pNA (Diapharma) for factor Xa and trypsin; H-(D)-Ile-Pro-Arg-pNA (Diapharma) for factor VIIa; H-(D)-CHT-Gly-Arg-pNA (American Diagnostica) for factor XIIa; H-(D)-Leu-Ph-Gly-Arg-AMC(7-amino-4-methylcoumarin) (Pentapharm) or H-(D)-Pro-Phe-Arg-pNA (Diapharma) for plasma kallikrein; MeO-Suc-Arg-Pro-Tyr-pNA (Diapharma) for chymotrypsin.

All assays were conducted at room temperature except where noted in 96-well microtiter plate spectrophotometers or spectrofluorimeters (Molecular Devices) with simultaneous measurement of enzyme activities in control and inhibitor containing solutions. Compounds were dissolved and diluted in DMSO and analyzed at a final concentration of 1% DMSO except where noted. Assays were initiated by adding enzyme to buffered solutions containing substrate in the presence or absence of inhibitor. Hydrolysis of the substrate resulted in the release of pNA (*p*-nitroaniline), which was monitored spectrophotometrically by measuring the increase in absorbance at 405 nm, or the release of AMC (7-amino-4-methylcoumarin), which was monitored spectrofluorometrically by measuring the increase in emission at 460 nm with excitation at 380 nm. The rate of absorbance or fluorescence change is proportional to enzyme activity. A decrease in the rate of absorbance or fluorescence change in the presence of inhibitor is indicative of enzyme inhibition. Assays were conducted under conditions of excess substrate and inhibitor over enzyme. The Michaelis constant,  $K_m$ , for substrate hydrolysis by each protease was determined by fitting data from independent measurements at several substrate concentrations to the Michaelis–Menten equation:

$$v = \frac{V_{\max}[S]}{K_m + [S]}$$

where  $v$  is the observed velocity of the reaction,  $V_{\max}$  is the maximal velocity,  $[S]$  is the concentration of substrate, and  $K_m$  is the Michaelis constant for the substrate.

Values of  $\text{IC}_{50}$  were determined by allowing the protease to react with the substrate in the presence of the inhibitor. Reactions were allowed to go for periods of 10–120 min (depending on the protease), and the velocities (rate of absorbance or fluorescence change versus time) were measured.

The following relationship was used to calculate  $\text{IC}_{50}$  values:

$$\frac{v_s}{v_o} = A + \frac{B - A}{1 + \left(\frac{\text{IC}_{50}}{I}\right)^n}$$

where  $v_o$  is the velocity of the control in the absence of inhibitor,  $v_s$  is the velocity in the presence of inhibitor,  $I$  is the concentration of inhibitor,  $A$  is the minimum activity remaining (usually locked at zero),  $B$  is the maximum activity remaining (usually locked at 1.0),  $n$  is the Hill coefficient, a measure of the number and cooperativity of potential inhibitor binding sites, and  $\text{IC}_{50}$  is the concentration of inhibitor that produces 50% inhibition.

When negligible enzyme inhibition was observed at the highest inhibitor concentration tested, the value assigned as a lower limit for  $\text{IC}_{50}$  is the value that would be obtained with either 25% or 50% inhibition at the highest inhibitor concentration. In all other cases  $\text{IC}_{50}$  values represent the average of duplicate determinations obtained over 8–11 concentrations. Competitive inhibition was assumed for all proteases.  $\text{IC}_{50}$  values were converted to  $K_i$  values by the following relationship:

$$K_i = \frac{\text{IC}_{50}}{1 + \frac{[S]}{K_m}}$$

**aPTT and PT in Vitro Coagulation Assays.** Standard clotting assays were performed in a temperature-controlled automated coagulation device (Sysmex CA-6000, Dade-Behring). Blood was obtained from healthy volunteers by venipuncture and anticoagulated with one-tenth volume 0.11 M buffered sodium citrate (Vacutainer, Becton Dickinson). Plasma was obtained after centrifugation at 2000g for 10 min and kept on ice prior to use. An initial stock solution of the inhibitor at 10 mM was prepared in DMSO. Subsequent dilutions were done in plasma. Clotting time was determined on control plasma and plasma containing up to seven different concentrations of inhibitor. The activated partial thromboplastin time (aPTT) was performed using Alexin (Trinity Biotech) according to the reagent instructions. Plasma (50  $\mu\text{L}$ ) was warmed to 37 °C for 1 min before adding aPTT reagent (50  $\mu\text{L}$ ). Two minutes later calcium chloride (50  $\mu\text{L}$ ) was added. The prothrombin time (PT) was performed using Thromboplastin C-Plus (Dade-Behring) according to the reagent instructions. Plasma (50  $\mu\text{L}$ ) was warmed to 37 °C for 3 min before adding PT reagent (100  $\mu\text{L}$ ). Determinations were performed in duplicate and expressed as a mean ratio of treated vs baseline control. The concentrations required to prolong clotting time by 2-fold ( $\text{EC}_{2x}$ ) were calculated by linear interpolation (Microsoft Excel, Redmond, WA, USA) and are expressed as total plasma concentrations, not final assay concentrations after addition of clotting assay reagents.

#### Recombinant FXI Catalytic Domain Cloning and Expression.

A gene encoding the expression of amino acids D357 to V607 of FXI catalytic domain with the following modifications was made: point mutations N473G, T475G to mitigate lattice hindrance, an N-terminal addition of MDDDD which improved solubility and handling of the protein, and a six membered poly-histidine tail on the C-terminus to enable metal chelation affinity chromatography (sequence 1). The gene was inserted into pET14b T7 expression plasmid (EMD-Millapore). The sequence confirmed plasmid was transformed into competent Origami B, BL21(DE3) *E. coli* cells. The catalytic domain of FXI has eight cysteines and four disulfide bonds. Use of Origami B enabled a small portion of the protein product to have the correctly

oxidized pairings of these cysteines, which are ultimately purified from mismatched cousins by selection on a benzamidinium affinity resin. Fermentation of cells was undertaken at 37 °C until the logarithmic growth phase was reached. Expression was induced with IPTG at 20 °C. Cells were harvested 12–16 h later by centrifugation, and the cell pellets were frozen for future use.

**Sequence 1.** The amino acid sequence 1 of the FXI catalytic domain used to clone and express the protein is the following:

MDDDDKMDNECTTKIKPR<sup>1</sup>IVGGTASVRGEWPWQVTLHT-TSPTQRHLCCGSIIGNQWILTAACHFYGVESPKILRVYSG-ILNQSEIKEDTSFFGVQEIIHDQYKMAESGYDIALKLE-TTVGYGDSQRPICLPSKGDRNVIYTDWCWVTGWGYRKLDRDK-IQNTLQKAKIPLVTNEECQKRYRGHKITHKMICAGYREGG-KDACKGDSGGPLSCKHNEVWHLVGITSWGEGCAQRERPGV-YTNVVEYVDWILEKTQAVHHHHHH

In the amino acid sequence, the  $\Delta$  denotes the thrombin activation cleavage site. Underlined amino acids are modifications and termini additions employed.

**Recombinant FXIa Catalytic Domain Purification.** An amount of 40 g of cells (wet packed cell weight) was thawed and suspended in 150 mL of lysis buffer (50 mM Na/KPO<sub>4</sub>, pH 8.0, 0.3 M NaCl, 20 mM imidazole) per gram of packed cells and lysed mechanically in an Emulsiflex homogenizer. The lysate suspension was clarified by centrifugation at 10 °C, and the supernatant was combined with 6 mL of Ni-NTA Superflow resin (Qiagen Inc.) pre-equilibrated with buffer A (50 mM Na/KPO<sub>4</sub>, pH 8.0, 0.3 M NaCl, and 20 mM imidazole) and the mixture incubated for 2 h at 4 °C. The mixture was then packed into a column and was washed with 50 mL of buffer A. Crude FXI catalytic domain protein was eluted from the column with the buffer A supplemented with 300 mM imidazole. Fractions containing the protein were identified by molecular weight using SDS–PAGE and were pooled and dialyzed overnight against buffer B (50 mM triethanolamine, 100 mM NaCl, 1 mM EDTA, pH 7.9) at 4 °C. The next morning, dextran sulfate sodium salt was added to a final concentration of 20  $\mu$ g/mL. Thrombin (1000 units; Calbiochem, catalog no. 605160) was added, and the mixture was incubated for 30 min at 37 °C to convert the FXI catalytic domain to the active form (FXIa catalytic domain). To arrest the reaction, polybrene and MgCl<sub>2</sub> were added up to 100  $\mu$ g/mL and 20 mM, respectively. Imidazole was then added up to 10 mM, and the solution was loaded onto a 5 mL column of Ni-NTA Superflow, washed with buffer A, and eluted in buffer A supplemented with 300 mM imidazole. Fractions containing FXIa catalytic domain as determined by SDS–PAGE were pooled and filtered. Final purification of FXIa catalytic domain from inactive contaminants was accomplished by loading the Ni-NTA eluate onto a 5 mL benzamidinium Sepharose (GE, Healthcare) column pre-equilibrated in 50 mM Tris, pH 7.4, 1 M NaCl, and the column was washed with this buffer until baseline was achieved. FXIa catalytic domain protein able to bind to benzamidinium was eluted in the same buffer supplemented with 40 mM benzamidinium sulfate. The purified yield from this process was 2–4 mg of protein.

**Formation of Crystals Using Purified Recombinant FXIa Catalytic Domain Complexed to Compound 11h or 16b.** Crystals of FXIa catalytic domain complexed to benzamidinium were grown at 4 °C by the hanging-drop vapor diffusion method. FXIa catalytic domain from the last step of purification (10 mg/mL) was saturated with benzamidinium. A solution of 0.2 M (NH<sub>4</sub>)<sub>2</sub>SO<sub>4</sub>, 25% polyethylene glycol methyl ether-2000, and 100 mM NaOAc, pH 4.6, was used as the precipitant. Benzamidinium was replaced by compound 11h or 16b by soaking the FXIa catalytic domain/benzamidinium crystals in a solution containing 2 mM replacement inhibitor in matched precipitant. Crystals were cryoprotected in 20% ethylene glycol for mounting prior to X-ray diffraction.

**X-ray Crystal Structure Data Collection and Structure Refinement (See Supporting Information for Tabulated Parameters).** Data for FXIa crystals in complex with compound 11h or 16b were collected at the Advanced Photon Source (APS) beamline 17-ID or in the laboratory. Raw data were processed with the program HKL2000.<sup>21</sup> The atomic coordinates of human factor XIa<sup>12</sup> were used as a search model. Original refinement was carried out with

CNX (Accelrys), and inhibitor restraint dictionaries were built with QUANTA (Accelrys), which was also used for modeling. Later the structures were re-refined using BUSTER/TNT<sup>22</sup> (GlobalPhasing, Ltd.), MakeTNT, or GRADE (GlobalPhasing, Ltd.) for inhibitor restraint dictionaries, and COOT<sup>23</sup> and PROCHECK<sup>24</sup> for modeling. The PDB deposition numbers for compounds 11h and 16b complexed to FXIa are 4TY6 and 4TY7, respectively.

**Molecular Modeling Studies.** Compounds 11a and 11h were docked into the crystal structure of FXIa complexed to compound 3 using Glide XP (Schrodinger LLC, New York, NY) and OPLS2001 force field. Twenty-five docked poses were requested as output and were visually inspected. Binding poses were selected from these sets based on previous knowledge of docking outcomes and SAR. Additional refinement was completed by minimizing the selected molecule poses using MacroModel (Schrodinger LLC, New York, NY) with the OPLS2001 force field constraining all atoms outside 5 Å from the ligand binding site.

**AV-Shunt Thrombosis Model.** For a full description of the model see Wong et al.<sup>18a</sup> Arterial blood from the femoral artery of anesthetized (ketamine, 50 mg/kg im, and xylazine, 10 mg/kg im; supplemented as needed) New Zealand male white rabbits was diverted through a PE60 cannula to a AV-shunt device, which is composed of a double tygon tubing with the inner tubing containing a 2.5 cm long 2-0 silk thread, and returned to the animal via a PE60 cannula inserted into the opposite femoral vein. Significant thrombus formation was initiated through contact with the silk thread. After 40 min the AV-shunt was disconnected from the arterial and venous catheters. The silk thread, which was covered with the thrombus, was removed and weighed. The thrombus weight formed on the thread was calculated by subtracting the average weight of a clean 2.5 cm long 2-0 silk thread. After obtaining the thrombus formation induced by the AV-shunt in the control period, the compound or vehicle was given as a bolus iv followed by a continuous iv infusion via the jugular vein started 30 min prior to the insertion of a new AV-shunt. The thrombus formation induced by the AV-shunt in the treatment period was measured as described above. Data are reported as % inhibition of thrombus formation in the treatment period versus in control period. Three doses of compound 16b were tested: 0.1 mg/kg + 0.16 mg kg<sup>-1</sup> h<sup>-1</sup>, 0.5 mg/kg + 0.8 mg kg<sup>-1</sup> h<sup>-1</sup>, 2.5 mg/kg + 4 mg kg<sup>-1</sup> h<sup>-1</sup> using a dosing vehicle of saline. The saline vehicle did not significantly alter the AV-shunt-induced thrombus formation. A total of three rabbits were used for each dose of 16b. The ID<sub>50</sub> represents the dose that produced 50% inhibition of thrombus formation and was estimated by linear regression.

**Preparation of Compounds 11a–s.** Compounds 11a–s were prepared by application of the methods described for the preparation of 11a. 11i–s required additional functional group transformations as described.

**(S)-tert-Butyl (2-Phenyl-1-(4-phenyl-1H-imidazol-2-yl)ethyl)-carbamate (9a).** To a solution of *N*-Boc-L-phenylalanine (7) (750 mg, 3.7 mmol) in 1:1 EtOH/H<sub>2</sub>O (7.4 mL) was added Cs<sub>2</sub>CO<sub>3</sub> (650 mg, 1.89 mmol). The reaction mixture was stirred at rt for 1 h. The solvent was removed under vacuum, and the solids were suspended in DMF (4.7 mL). 2-Bromoacetophenone (1.0 g, 3.77 mmol) was added in a single portion, and the reaction mixture was stirred at rt for 1.5 h. The mixture was filtered to remove solids. The solids were washed with DMF. The combined washings and filtrate were concentrated in vacuo to yield (S)-2-oxo-2-phenylethyl 2-((*tert*-butoxycarbonyl)-amino)-3-phenylpropanoate (I-1) (650 mg). I-1 was placed in a flask fitted with a Dean–Stark trap and dissolved in xylenes (10 mL). NH<sub>4</sub>OAc (2.64 g, 30 mmol) was added to the flask, and the mixture was heated to reflux for 3 h. The reaction mixture was cooled to rt and the solvent removed in vacuo. The residue was redissolved in EtOAc, washed with saturated aq NaHCO<sub>3</sub> and brine, dried over Na<sub>2</sub>SO<sub>4</sub>, filtered, and evaporated in vacuo to provide 9a (780 mg, 57%). *m/z* 364 [M + H]<sup>+</sup>. Alternatively, I-1 and 10 equiv of NH<sub>4</sub>OAc were dissolved in ethanol and heated to 160 °C in a sealed tube for 30 min using microwave irradiation. The reaction was cooled to rt, the ethanol was evaporated in vacuo, and the residue was redissolved in EtOAc. The organic layer was washed with brine, dried over MgSO<sub>4</sub>, and



evaporated to dryness. The product thus formed was sufficiently pure to carry onto the next step.

**tert-Butyl ((trans-4-(((S)-2-Phenyl-1-(4-phenyl-1H-imidazol-2-yl)ethyl)carbamoyl)cyclohexyl)methyl)carbamate (10a).** To a solution of 9a (100 mg, 0.28 mmol) in CH<sub>2</sub>Cl<sub>2</sub> (2.8 mL) was added neat TFA (0.2 mL). The reaction mixture was stirred at rt for 16 h. The solvent and TFA were removed in vacuo. The residue was twice redissolved in CH<sub>3</sub>OH and the solvent removed in vacuo to provide (S)-2-phenyl-1-(4-phenyl-1H-imidazol-2-yl)ethanamine, bis-trifluoroacetic acid salt (**I-2**) (124 mg, 92%), which was carried onto the next step without purification. *m/z* 262 [M - H]<sup>+</sup>. To a solution of **I-2** (75 mg, 0.15 mmol) and *N*-Boc-tranexamic acid (75 mg, 0.29 mmol) in pyridine (1.7 mL) was added BOP reagent (152 mg, 0.34 mmol). The reaction mixture was stirred at rt for 12 h. The mixture was diluted with H<sub>2</sub>O and extracted with EtOAc. The combined organic extracts were washed with brine, dried over Na<sub>2</sub>SO<sub>4</sub>, filtered, and evaporated in vacuo to give **10a** (100 mg, 71%). **10a** was carried onto the next step without purification. *m/z* 503 [M + H]<sup>+</sup>. Alternatively, **I-2** was coupled with 1.0 equiv of *N*-Boc-tranexamic acid, 1.2 equiv of HOAt, 5.0 equiv of *N*-methylmorpholine, and 1.2 equiv of EDC.

**trans-4-(Aminomethyl)-*N*-((S)-2-phenyl-1-(4-phenyl-1H-imidazol-2-yl)ethyl)cyclohexanecarboxamide, Bis-trifluoroacetic Acid Salt (11a).** **10a** (100 mg, 0.20 mmol) was dissolved in 30% TFA in CH<sub>2</sub>Cl<sub>2</sub> (2.0 mL). The reaction mixture was stirred at rt for 3 h. The mixture was twice dissolved in toluene and dried in vacuo. **11a** was isolated by preparative HPLC (46 mg, 49%). <sup>1</sup>H NMR (500 MHz, CD<sub>3</sub>OD) δ 1.02–1.11 (m, 2H), 1.32–1.45 (m, 2H), 1.54–1.61 (m, 1H), 1.80 (br d, *J* = 12 Hz, 1H), 1.86 (br d, *J* = 12 Hz, 3H), 2.28 (dt, *J* = 12, 3.3 Hz, 1H), 2.77 (d, *J* = 7.1 Hz, 2H), 3.31 (dd, 1H, overlap with CH<sub>3</sub>OH), 3.38 (dd, *J* = 13, 8.0 Hz), 5.31 (t, *J* = 8.2 Hz, 1H), 7.18 (d, *J* = 7.1 Hz, 2H), 7.22–7.30 (m, 3H), 7.43–7.50 (m, 3H), 7.62 (d, *J* = 6.6 Hz, 2H), 7.75 (s, 1H). *m/z* 403 [M + H]<sup>+</sup>.

**trans-4-(Aminomethyl)-*N*-((S)-1-(4-(4-cyanophenyl)-1H-imidazol-2-yl)-2-phenylethyl)cyclohexanecarboxamide, Bis-trifluoroacetic Acid Salt (11b).** <sup>1</sup>H NMR (500 MHz, CD<sub>3</sub>OD) δ 1.02–1.12 (m, 2H), 1.30–1.46 (m, 2H), 1.53–1.61 (m, 1H), 1.80 (d, *J* = 12 Hz, 1H), 1.86 (d, *J* = 11 Hz, 3H), 2.23–2.32 (m, 1H), 2.64 (d, *J* = 9.4 Hz, 1H), 2.78 (d, *J* = 6.6 Hz, 2H), 3.32 (dd, *J* = 8.2 Hz, 1 H, overlap with CH<sub>3</sub>OH), 3.38 (dd, *J* = 13, 8.2 Hz, 1H), 5.33 (t, *J* = 8.2 Hz, 1H), 7.19 (d, *J* = 6.6 Hz, 2H), 7.22–7.26 (m, 1H), 7.26–7.32 (m, 2H), 7.85 (s, 4H), 7.94 (s, 1H). HRMS calcd for C<sub>26</sub>H<sub>29</sub>N<sub>5</sub>O [M + H]<sup>+</sup> 428.2450, found 428.2443.

**Methyl 4-(2-((S)-1-(trans-4-(Aminomethyl)cyclohexanecarboxamido)-2-phenylethyl)-1H-imidazol-4-yl)cyclohexanecarboxamide, Bis-trifluoroacetic Acid Salt (11c).** <sup>1</sup>H NMR (500 MHz, CD<sub>3</sub>OD) δ 1.00–1.14 (m, 2H), 1.30–1.47 (m, 2H), 1.51–1.64 (m, 1H), 1.80 (d, *J* = 12 Hz, 1H), 1.86 (d, *J* = 12 Hz, 3H), 2.23–2.34 (m, 1H), 2.78 (d, *J* = 6.6 Hz, 2H), 3.32 (dd, *J* = 8.2 Hz, 1 H, overlap with CH<sub>3</sub>OH), 3.39 (dd, *J* = 13, 8.2 Hz, 1H), 3.93 (s, 3H), 5.33 (t, *J* = 8.2 Hz, 1H), 7.19 (d, *J* = 7.2 Hz, 2H), 7.22–7.26 (m, 1H), 7.27–7.32 (m, 2H), 7.78 (d, *J* = 8.8 Hz, 2H), 7.90 (s, 1H), 8.12 (d, *J* = 8.8 Hz, 2H). HRMS calcd for C<sub>27</sub>H<sub>32</sub>N<sub>4</sub>O<sub>3</sub> [M + H]<sup>+</sup> 461.2553, found 461.2570.

**Ethyl 2-(4-(2-((S)-1-(trans-4-(Aminomethyl)cyclohexanecarboxamido)-2-phenylethyl)-1H-imidazol-4-yl)phenyl)acetate, Bis-trifluoroacetic Acid Salt (11d).** <sup>1</sup>H NMR (500 MHz, CD<sub>3</sub>OD) δ 1.01–1.13 (m, 2H), 1.24 (t, *J* = 7.1 Hz, 3H), 1.33–1.44 (m, 2H), 1.51–1.64 (m, 1H), 1.80 (d, *J* = 13 Hz, 1H), 1.86 (d, *J* = 11 Hz, 4H), 2.23–2.32 (m, 1H), 2.77 (d, *J* = 7.1 Hz, 2H), 3.32–3.38 (dd, 1H, overlap with CH<sub>3</sub>OH), 3.38 (dd, *J* = 13, 8.2, 1H), 3.70 (s, 2H), 4.15 (q, *J* = 7.2 Hz, 2H), 5.31 (t, *J* = 8.5 Hz, 1H), 7.17 (d, *J* = 7.2 Hz, 2H), 7.21–7.26 (m, 1H), 7.27–7.32 (m, 2H), 7.41 (d, *J* = 8.2 Hz, 2H), 7.59 (d, *J* = 8.2 Hz, 2H), 7.74 (s, 1H). HRMS for calcd for C<sub>29</sub>H<sub>36</sub>N<sub>4</sub>O<sub>3</sub> [M + H]<sup>+</sup> 489.2866, found 489.2861.

**trans-4-(Aminomethyl)-*N*-((S)-1-(4-(3-cyanophenyl)-1H-imidazol-2-yl)-2-phenylethyl)cyclohexanecarboxamide, Bis-trifluoroacetic Acid Salt (11e).** <sup>1</sup>H NMR (500 MHz, CD<sub>3</sub>OD) δ 0.99–1.13 (m, 2H), 1.26–1.47 (m, 2H), 1.52–1.63 (m, 1H), 1.79 (d, *J* = 12 Hz, 1H), 1.85 (d, *J* = 12 Hz, 3H), 2.21–2.34 (m, 1H), 2.77 (d, *J* = 7.1 Hz, 2H), 3.32 (dd, *J* = 8.0 Hz, 1 H, overlap with CH<sub>3</sub>OH), 3.38 (m, *J* = 13, 8.2 Hz, 1H), 5.34 (t, *J* = 8.2 Hz, 1H), 7.19 (d, *J* = 7.1 Hz,

2H), 7.22–7.26 (m, 1H), 7.27–7.32 (m, 2H), 7.68 (t, *J* = 8.0 Hz, 1H), 7.81 (d, *J* = 7.7 Hz, 1H), 7.91 (s, 1H), 7.97 (d, *J* = 7.7 Hz, 1H), 8.07 (s, 1H). *m/z* 428 [M + H]<sup>+</sup>.

**Ethyl 2-(3-(2-((S)-1-(trans-4-(Aminomethyl)cyclohexanecarboxamido)-2-phenylethyl)-1H-imidazol-4-yl)phenyl)acetate, Bis-trifluoroacetic Acid Salt (11f).** <sup>1</sup>H NMR (500 MHz, CD<sub>3</sub>OD) δ 1.02–1.12 (m, 2H), 1.25 (t, *J* = 7.2 Hz, 3H), 1.33–1.46 (m, 2H), 1.57 (m, 1H), 1.80 (d, *J* = 12 Hz, 1H), 1.86 (d, *J* = 12 Hz, 3H), 2.23–2.32 (m, 1H), 2.77 (d, 2H), 3.30 (dd, 1H, overlap with CH<sub>3</sub>OH), 3.38 (dd, *J* = 13, 8.2 Hz, 1H), 3.72 (s, 2H), 4.15 (q, *J* = 7.2 Hz, 2H), 5.31 (t, *J* = 8.2 Hz, 1H), 7.16–7.21 (m, 2H), 7.25 (d, *J* = 5.5 Hz, 1H), 7.26–7.32 (m, 2H), 7.37–7.41 (m, 1H), 7.46 (t, *J* = 7.7 Hz, 1H), 7.52–7.58 (m, 2H), 7.76 (s, 1H). *m/z* 489 [M + H]<sup>+</sup>.

**trans-4-(Aminomethyl)-*N*-((S)-2-phenyl-1-(4-(4-sulfamoylphenyl)-1H-imidazol-2-yl)ethyl)cyclohexanecarboxamide, Bis-trifluoroacetic Acid Salt (11g).** <sup>1</sup>H NMR (500 MHz, CD<sub>3</sub>OD) δ 1.00–1.12 (m, 2H), 1.30–1.47 (m, 2H), 1.51–1.63 (m, 1H), 1.79 (d, *J* = 12 Hz, 1H), 1.86 (d, *J* = 10 Hz, 3H), 2.21–2.33 (m, 1H), 2.77 (d, *J* = 7.2 Hz, 2H), 3.31 (dd, *J* = 8.25 Hz, 1H, overlap with CH<sub>3</sub>OH), 3.38 (dd, *J* = 13, 8.2 Hz, 1H), 5.32 (t, *J* = 8.2 Hz, 1H), 7.19 (d, *J* = 7.2 Hz, 2H), 7.21–7.26 (m, 1H), 7.26–7.32 (m, 2H), 7.82 (d, *J* = 8.2 Hz, 2H), 7.89 (s, 1H), 7.99 (d, *J* = 8.8 Hz, 2H). *m/z* 482 [M + H]<sup>+</sup>.

**tert-Butyl ((trans-4-(((S)-1-(4-(4-carbamoylphenyl)-1H-imidazol-2-yl)-2-phenylethyl)carbamoyl)cyclohexyl)methyl)carbamate (10h).** **10b** (117 mg, 0.22 mmol) was dissolved in DMSO (2 mL) and treated with K<sub>2</sub>CO<sub>3</sub> (90.0 mg, 0.65 mmol) under Ar. 30% aq H<sub>2</sub>O<sub>2</sub> (0.8 mL, 2.4 mmol) and MgO (44 mg, 1.11 mmol) were added sequentially. The reaction mixture was stirred at rt for 4 h. The reaction mixture was diluted with EtOAc, washed with 1 N aq HCl and brine, dried over MgSO<sub>4</sub>, filtered, and evaporated to dryness in vacuo to provide **10h** (109 mg, 90%) as a yellow solid. **10h** was carried onto the next step without purification. *m/z* 546 [M + H]<sup>+</sup>.

**4-(2-((S)-1-(trans-4-(Aminomethyl)cyclohexanecarboxamido)-2-phenylethyl)-1H-imidazol-4-yl)benzamide, Bis-trifluoroacetic Acid Salt (11h).** **10h** was treated with TFA according to the procedure described for the conversion of compound **10a** to **11a** to provide **11h** (17.3 mg, 20%). <sup>1</sup>H NMR (500 MHz, CD<sub>3</sub>OD) δ 1.00–1.13 (m, 2H), 1.30–1.47 (m, 2H), 1.52–1.63 (m, 1H), 1.80 (d, *J* = 12 Hz, 1H), 1.86 (d, *J* = 11 Hz, 3H), 2.28 (t, *J* = 12 Hz, 1H), 2.77 (d, *J* = 6.6 Hz, 2H), 3.31 (dd, *J* = 8.8 Hz, 1H, overlap with CH<sub>3</sub>OH), 3.38 (dd, *J* = 13, 8.2 Hz, 1H), 5.33 (t, *J* = 8.2 Hz, 1H), 7.19 (d, *J* = 7.2 Hz, 2H), 7.21–7.26 (m, 1H), 7.26–7.32 (m, 2H), 7.76 (d, *J* = 8.8 Hz, 2H), 7.88 (s, 1H), 7.99 (d, *J* = 8.2 Hz, 2H). HRMS calcd for C<sub>26</sub>H<sub>30</sub>N<sub>5</sub>O<sub>2</sub> [M + H]<sup>+</sup> 446.2556, found 446.2561.

**tert-Butyl ((trans-4-(((S)-1-(5-bromo-4-(4-carbamoylphenyl)-1H-imidazol-2-yl)-2-phenylethyl)carbamoyl)cyclohexyl)methyl)carbamate (10i).** To a solution of **10h** (70 mg, 0.13 mmol) in CHCl<sub>3</sub> (10 mL) was added bromine (21 mg, 0.13 mmol). The reaction mixture was stirred at rt for 16 h. The reaction mixture was evaporated to dryness in vacuo to yield **10i** (93 mg, 100%), which was carried onto the next step without purification. *m/z* 622/624 (1:1) [M - H]<sup>+</sup>.

**4-(2-((S)-1-(trans-4-(Aminomethyl)cyclohexanecarboxamido)-2-phenylethyl)-5-bromo-1H-imidazol-4-yl)benzamide, Bis-trifluoroacetic Acid Salt (11i).** **10i** was converted to **11i** (35.8 mg, 36%) using the method described for the conversion of compound **10a** to **11a**. <sup>1</sup>H NMR (500 MHz, CD<sub>3</sub>OD) δ 0.99–1.11 (m, 2H), 1.29–1.48 (m, 2H), 1.55–1.63 (m, 1H), 1.75 (d, 1H), 1.85 (d, *J* = 9.9 Hz, 3H), 2.16–2.27 (m, 1H), 2.77 (d, *J* = 6.6 Hz, 2H), 3.17 (dd, *J* = 13, 8.2 Hz, 1H), 3.25 (dd, *J* = 13, 7.7 Hz, 1H), 3.98 (s, 1H), 5.22 (t, *J* = 7.7 Hz, 1H), 7.17 (d, *J* = 7.2 Hz, 2H), 7.20 (d, *J* = 7.2 Hz, 1H), 7.23–7.28 (m, 2H), 7.75 (d, *J* = 8.2 Hz, 2H), 7.94 (d, *J* = 8.2 Hz, 2H). HRMS calcd for C<sub>26</sub>H<sub>30</sub>BrN<sub>5</sub>O<sub>2</sub> 524.1661 [M + H]<sup>+</sup>, found 524.1653.

**4-(2-((S)-1-(trans-4-(Aminomethyl)cyclohexanecarboxamido)-2-phenylethyl)-5-chloro-1H-imidazol-4-yl)benzamide, Bis-trifluoroacetic Acid Salt (11j).** **9b** was converted to **11j** by sequentially applying the procedures used to convert **10b** to **10h**, **14a** to **14b**, and **9a** to **11a**. <sup>1</sup>H NMR (400 MHz, CD<sub>3</sub>OD) δ 0.94–1.13 (m, 2H), 1.30–1.49 (m, 2H), 1.51–1.64 (m, 1H), 1.75 (d, *J* = 13 Hz, 1H), 1.86 (d, *J* = 11 Hz, 3H), 2.16–2.27 (m, 1H), 2.77 (d, *J*

= 7.0 Hz, 2H), 3.14 (dd,  $J = 13$ , 7.2 Hz, 1H), 3.24 (dd,  $J = 13$ , 7.5 Hz, 1H), 5.21 (t,  $J = 7.9$  Hz, 1H), 7.14–7.22 (m, 3H), 7.22–7.29 (m, 2H), 7.74 (d,  $J = 8.8$  Hz, 2H), 7.93 (d,  $J = 8.8$  Hz, 2H).  $m/z$  480  $[M + H]^+$ .

**4-(2-((S)-1-(trans-4-(Aminomethyl)cyclohexanecarboxamido)-2-phenylethyl)-5-fluoro-1H-imidazol-4-yl)-benzamide, Bis-trifluoroacetic Acid Salt (11k).** 10h was converted to 11k by sequential application of the methods described for the conversion of 14a to 14c and 10a to 11a.  $^1\text{H}$  NMR (400 MHz,  $\text{CD}_3\text{OD}$ )  $\delta$  7.90 (d,  $J = 8.2$  Hz, 2H), 7.58 (d,  $J = 8.2$  Hz, 2H), 7.27–7.20 (m, 2H), 7.20–7.14 (m, 3H), 5.17 (t,  $J = 7.7$  Hz, 1H), 3.20 (dd,  $J = 13.2$ , 7.7 Hz, 1H), 3.12 (dd,  $J = 13.2$ , 7.7 Hz, 1H), 2.77 (d,  $J = 7.1$  Hz, 2H), 2.26–2.16 (m, 1H), 1.89–1.80 (m, 3H), 1.78–1.70 (m, 1H), 1.64–1.51 (m, 1H), 1.49–1.29 (m, 2H), 1.12–0.98 (m, 2H).  $^{19}\text{F}$  NMR (376 MHz,  $\text{CD}_3\text{OD}$ )  $\delta$  -77.47 (s), -133.62 (s).  $m/z$  464  $[M + H]^+$ .

**4-(2-((S)-1-(trans-4-(tert-Butoxycarbonylamino)methyl)-cyclohexanecarboxamido)-2-phenylethyl)-1H-imidazol-4-yl)-benzoic Acid (10l).** To a solution of 10c (162 mg, 0.28 mmol) in  $\text{CH}_3\text{OH}$  (5 mL) and EtOAc (1 mL) were added 1 N aq NaOH (2 mL) and MgO (112 mg, 2.8 mmol). The reaction mixture was stirred for 5 h at rt. The solvent was evaporated to dryness in vacuo. The residue was diluted with water and treated with 1 N aq HCl. The aqueous solution was diluted with EtOAc, washed with brine, dried over  $\text{MgSO}_4$ , filtered, and evaporated in vacuo to yield 10l (75 mg, 60%), which was carried onto the next step without purification.  $m/z$  548  $[M + H]^+$ .

**4-(2-((S)-1-(trans-4-(Aminomethyl)cyclohexanecarboxamido)-2-phenylethyl)-1H-imidazol-4-yl)benzoic Acid, Bis-trifluoroacetic Acid Salt (11l).** 10l was treated according to the method described for compound the conversion of compound 10a to 11a to provide 11l (34 mg, 18%).  $^1\text{H}$  NMR (500 MHz,  $\text{CD}_3\text{OD}$ )  $\delta$  1.02–1.11 (m, 2H), 1.32–1.46 (m, 2H), 1.53–1.62 (m, 1H), 1.80 (d,  $J = 12$  Hz, 1H), 1.86 (d,  $J = 12$  Hz, 3H), 2.28 (tt,  $J = 12$ , 3.3 Hz, 1H), 2.77 (d,  $J = 7.1$  Hz, 2H), 3.33 (d,  $J = 8.2$  Hz, 1 H, overlap with  $\text{CH}_3\text{OH}$ ), 3.39 (dd,  $J = 13$ , 8.2 Hz, 1H), 5.33 (t,  $J = 8.2$  Hz, 1H), 7.19 (d,  $J = 7.1$  Hz, 2H), 7.24 (t,  $J = 7.1$  Hz, 1H), 7.29 (t,  $J = 7.1$  Hz, 2H), 7.76 (d,  $J = 8.2$  Hz, 2H), 7.89 (s, 1H), 8.12 (d,  $J = 8.8$  Hz, 2H). HRMS calcd for  $\text{C}_{26}\text{H}_{29}\text{N}_4\text{O}_3$  447.2396  $[M + H]^+$ , found 447.2397.

**tert-Butyl ((trans-4-((S)-1-(4-(4-(Methylcarbamoyl)phenyl)-1H-imidazol-2-yl)-2-phenylethyl)carbamoyl)cyclohexyl)-methylcarbamate (10m).** 10l (45 mg, 0.08 mmol) and methylamine (0.2 mL, 0.09 mmol) were converted to 10m (44.0 mg, 93%) using the alternative procedure described for conversion of I-2 to 10a. 10m was carried to the next step without purification.  $m/z$  560  $[M + H]^+$ .

**4-(2-((S)-1-(trans-4-(Aminomethyl)cyclohexanecarboxamido)-2-phenylethyl)-1H-imidazol-4-yl)-N-methylbenzamide, Bis-trifluoroacetic Acid Salt (11m).** 10m was converted to 11m (1.0 mg, 3%) according to the method for the conversion of 10a to 11a.  $^1\text{H}$  NMR (500 MHz,  $\text{CD}_3\text{OD}$ )  $\delta$  1.02–1.11 (m, 1H), 1.32–1.46 (m, 1H), 1.53–1.62 (m, 1H), 1.79 (d,  $J = 13$  Hz, 1H), 1.86 (d,  $J = 11$  Hz, 1H), 2.30–2.65 (m, 1H), 2.77 (d,  $J = 7.2$  Hz, 1H), 2.92 (s, 3H), 3.38 (dd,  $J = 13$ , 8.2 Hz, 2H, overlap with  $\text{CH}_3\text{OH}$ ), 5.29 (t,  $J = 8.2$  Hz, 1H), 7.16 (d,  $J = 7.2$  Hz, 1H), 7.23 (t,  $J = 7.2$  Hz, 1H), 7.28 (t,  $J = 7.2$  Hz, 1H), 7.72 (d,  $J = 8.2$  Hz, 1H), 7.86 (s, 1H), 7.92 (d,  $J = 8.8$  Hz, 1H). HRMS calcd for  $\text{C}_{27}\text{H}_{32}\text{N}_5\text{O}_2$  460.2713  $[M + H]^+$ , found 460.2735.

**4-(2-((S)-1-(trans-4-(Aminomethyl)cyclohexanecarboxamido)-2-phenylethyl)-1H-imidazol-4-yl)-N,N-dimethylbenzamide, Bis-trifluoroacetic Acid Salt (11n).** 11n was prepared from 10l according to the method for 11m from 10l by substituting dimethylamine for methylamine.  $^1\text{H}$  NMR (500 MHz,  $\text{CD}_3\text{OD}$ )  $\delta$  1.03–1.11 (m, 2H), 1.32–1.46 (m, 2H), 1.54–1.61 (m, 1H), 1.81 (d,  $J = 15$  Hz, 1H), 1.86 (d,  $J = 10$  Hz, 3H), 2.28 (tt,  $J = 12$ , 3.3 Hz, 1H), 2.77 (d,  $J = 7.1$  Hz, 2H), 3.01 (s, 3H), 3.12 (s, 3H), 3.31 (dd, 1 H, overlap with  $\text{CH}_3\text{OH}$ ), 3.39 (dd,  $J = 13$ , 8.2 Hz, 1H), 5.31 (t,  $J = 8.2$  Hz, 1H), 7.18 (d,  $J = 7.2$  Hz, 2H), 7.24 (t,  $J = 7.2$  Hz, 1H), 7.29 (t,  $J = 7.4$  Hz, 2H), 7.55 (d,  $J = 8.2$  Hz, 2H), 7.72 (d,  $J = 8.2$  Hz, 2H), 7.85 (s, 1H) ppm. HRMS calcd for  $\text{C}_{28}\text{H}_{34}\text{N}_5\text{O}_2$  474.2870  $[M + H]^+$ , found 474.2875.

**2-(4-(2-((S)-1-(trans-4-(tert-Butoxycarbonylamino)methyl)-cyclohexanecarboxamido)-2-phenylethyl)-1H-imidazol-4-yl)-phenyl)acetic Acid (10o).** 10d (200 mg, 0.34 mmol) was dissolved in  $\text{CH}_3\text{OH}$  (3 mL) and treated with 1 N aq NaOH (0.34 mL, 0.34 mmol). The reaction mixture was stirred at rt for 16 h. The solvent was removed in vacuo. The residue purified by preparative HPLC to provide 10o (90 mg, 47%).  $m/z$  561  $[M + H]^+$ .

**2-(4-(2-((S)-1-(trans-4-(Aminomethyl)cyclohexanecarboxamido)-2-phenylethyl)-1H-imidazol-4-yl)phenyl)acetic Acid, Bis-trifluoroacetic Acid Salt (11o).** 10o was treated according to the method described for conversion of 10a to 11a to provide 11o (15 mg, 81%).  $^1\text{H}$  NMR (500 MHz,  $\text{CD}_3\text{OD}$ )  $\delta$  0.99–1.13 (m, 2H), 1.52–1.63 (m, 1H), 1.80 (d,  $J = 12$  Hz, 1H), 1.86 (d,  $J = 10$  Hz, 3H), 2.22–2.33 (m, 1H), 2.77 (d,  $J = 7.2$  Hz, 2H), 3.31 (dd, 1 H, overlap with  $\text{CH}_3\text{OH}$ ), 3.38 (dd,  $J = 13$ , 8.2 Hz, 1H), 3.67 (s, 2H), 5.31 (t,  $J = 8.2$  Hz, 1H), 7.18 (d,  $J = 6.6$  Hz, 2H), 7.21–7.26 (m, 1H), 7.26–7.32 (m, 2H), 7.42 (d,  $J = 8.2$  Hz, 2H), 7.59 (d,  $J = 8.2$  Hz, 2H), 7.74 (s, 1H). HRMS calcd for  $\text{C}_{27}\text{H}_{32}\text{N}_4\text{O}_3$  461.2553  $[M + H]^+$ , found 461.2572.

**tert-Butyl (trans-4-((S)-1-(4-(4-(2-Amino-2-oxoethyl)-phenyl)-1H-imidazol-2-yl)-2-phenylethyl)carbamoyl)-cyclohexyl)carbamate (10p).** To a solution of 10o (33 mg, 0.060 mmol) and HOAc (9.7 mg, 0.071 mmol) in DMF (1 mL) were added sequentially N-methylmorpholine (18.2 mg, 0.18 mmol) and EDC (13.6 mg, 0.071 mmol). The reaction mixture was stirred for 30 min at rt. Concentrated aq  $\text{NH}_3$  (5 drops from a Pasteur pipet) was added, and the reaction mixture was stirred at rt for 16 h. The mixture was diluted with EtOAc and washed with a 1:1 mixture of  $\text{H}_2\text{O}$  and brine, 1 N aq HCl, and brine, dried over  $\text{MgSO}_4$ , filtered, and dried in vacuo. The product was isolated by preparative HPLC to provide 10p (9 mg, 22%).  $m/z$  560  $[M + H]^+$ .

**trans-N-((S)-1-(4-(4-(2-Amino-2-oxoethyl)phenyl)-1H-imidazol-2-yl)-2-phenylethyl)-4-(aminomethyl)cyclohexanecarboxamide, Bis-trifluoroacetic Acid Salt (11p).** 10p (9 mg, 0.016 mmol) was converted to 11p (11 mg, 99%) according to the method described for the conversion of compound 10a to 11a.  $^1\text{H}$  NMR (500 MHz,  $\text{CD}_3\text{OD}$ )  $\delta$  1.02–1.11 (m, 2H), 1.32–1.44 (m, 2H), 1.53–1.61 (m, 1H), 1.79 (d,  $J = 13$  Hz, 1H), 1.85 (d,  $J = 11$  Hz, 3H), 2.28 (tt,  $J = 3.0$ , 12 Hz, 1H), 2.77 (d,  $J = 7.2$  Hz, 2H), 3.31 (dd, 1 H, overlap with  $\text{CH}_3\text{OH}$ ), 3.38 (dd,  $J = 13$ , 8.0 Hz, 1H), 3.57 (s, 2H), 5.31 (t,  $J = 8.2$  Hz, 1H), 7.17 (d,  $J = 7.2$  Hz, 2H), 7.22–7.25 (m, 1H), 7.27–7.30 (m, 2H), 7.43 (d,  $J = 8.2$  Hz, 2H), 7.59 (d,  $J = 8.2$  Hz, 2H), 7.74 (s, 1H). HRMS calcd for  $\text{C}_{27}\text{H}_{33}\text{N}_5\text{O}_2$  460.2713  $[M + H]^+$ , found 460.2714.

**3-(2-((S)-1-(trans-4-(Aminomethyl)cyclohexanecarboxamido)-2-phenylethyl)-1H-imidazol-4-yl)benzamide, Bis-trifluoroacetic Acid Salt (11q).** 11q was prepared from 10e according to the method used for conversion of 10b to 11h.  $^1\text{H}$  NMR (500 MHz,  $\text{CD}_3\text{OD}$ )  $\delta$  1.00–1.13 (m, 2H), 1.30–1.47 (m, 2H), 1.52–1.64 (m, 1H), 1.80 (d,  $J = 12$  Hz, 1H), 1.86 (d,  $J = 12$  Hz, 3H), 2.28 (t,  $J = 12$  Hz, 1H), 2.77 (d,  $J = 7.2$  Hz, 2H), 3.32 (dd,  $J = 8.2$  Hz, overlap with  $\text{CH}_3\text{OH}$ ), 3.39 (dd,  $J = 13$ , 8.2 Hz, 1H), 5.34 (t,  $J = 8.2$  Hz, 1H), 7.19 (d,  $J = 6.6$  Hz, 2H), 7.22–7.26 (m, 1H), 7.27–7.32 (m, 2H), 7.60 (t,  $J = 7.7$  Hz, 1H), 7.83 (s, 1H), 7.93 (d,  $J = 8.2$  Hz, 1H), 8.18 (s, 1H). HRMS calcd for  $\text{C}_{26}\text{H}_{31}\text{N}_5\text{O}_2$  446.2556  $[M + H]^+$ , found 446.2535.

**2-(3-(2-((S)-1-(trans-4-(Aminomethyl)cyclohexanecarboxamido)-2-phenylethyl)-1H-imidazol-4-yl)phenyl)acetic Acid, Bis-trifluoroacetic Acid Salt (11r).** 11r was synthesized from 10f using the methods for the conversion of 10d to 11o.  $^1\text{H}$  NMR (500 MHz,  $\text{CD}_3\text{OD}$ )  $\delta$  1.01–1.13 (m, 2H), 1.29–1.47 (m, 2H), 1.52–1.63 (m, 1H), 1.80 (d,  $J = 12$  Hz, 1H), 1.86 (d,  $J = 10$  Hz, 4H), 2.23–2.32 (m,  $J = 12$ , 12, 3.1, 3.0 Hz, 1H), 2.77 (d,  $J = 7.2$  Hz, 2H), 3.31 (dd, 1H, overlap with  $\text{CH}_3\text{OH}$ ), 3.38 (dd,  $J = 13$ , 8.2 Hz, 1H), 5.31 (t,  $J = 8.2$  Hz, 1H), 7.18 (d,  $J = 7.2$  Hz, 2H), 7.22–7.27 (m, 1H), 7.27–7.32 (m, 2H), 7.39 (d,  $J = 7.7$  Hz, 1H), 7.45 (t,  $J = 7.7$  Hz, 1H), 7.53 (d,  $J = 7.7$  Hz, 1H), 7.56 (s, 1H), 7.76 (s, 1H).  $m/z$  461  $[M + H]^+$ .

**trans-N-((S)-1-(4-(3-(2-Amino-2-oxoethyl)phenyl)-1H-imidazol-2-yl)-2-phenylethyl)-4-(aminomethyl)cyclohexanecarboxamide, Bis-trifluoroacetic Acid Salt (11s).** 11s was synthesized from 10f using the methods for the conversion of 10d



to **11p**.  $^1\text{H}$  NMR (500 MHz,  $\text{CD}_3\text{OD}$ )  $\delta$  0.99–1.13 (m, 2H), 1.29–1.48 (m, 2H), 1.53–1.62 (m, 1H), 1.80 (d, 1H), 1.86 (d,  $J = 10$  Hz, 3H), 2.21–2.33 (m, 1H), 2.77 (d,  $J = 7.2$  Hz, 2H), 3.33 (dd, 1H, overlap with  $\text{CH}_3\text{OH}$ ), 3.38 (dd,  $J = 13$ , 8.2 Hz, 1H), 3.59 (s, 2H), 5.32 (t,  $J = 8.2$  Hz, 1H), 7.18 (d,  $J = 7.15$  Hz, 2H), 7.22–7.26 (m, 1H), 7.26–7.32 (m, 2H), 7.37–7.41 (m, 1H), 7.45 (t,  $J = 7.7$  Hz, 1H), 7.52 (d, 1H), 7.57 (s, 1H), 7.75 (s, 1H).  $m/z$  460  $[\text{M} + \text{H}]^+$ .

**4-(2-Bromoacetyl)-2-fluorobenzonitrile (13).** 4-Bromo-3-fluorobenzoic acid (**12**) (7.5 g, 34 mmol),  $\text{Zn}(\text{CN})_2$  (4.0 g, 34 mmol), and  $\text{Pd}(\text{PPh}_3)_4$  (3.95 g, 34 mmol) were combined in 60 mL of DMF that had been sparged with  $\text{N}_2$ . The reaction mixture was heated at  $90^\circ\text{C}$  under  $\text{N}_2$  for 3 h. The mixture was cooled to rt and filtered. The filtrate was diluted with water and extracted with EtOAc. The combined organic layers were washed with  $\text{H}_2\text{O}$ , brine, dried over  $\text{MgSO}_4$ , and concentrated in vacuo to yield 4-cyano-3-fluorobenzoic acid (**I-3**) (4.0 g, 20 mmol). To a solution of **I-3** in  $\text{CH}_2\text{Cl}_2$  (50 mL) was added oxalyl chloride (2.3 mL, 26 mmol) dropwise over 15 min. The reaction mixture was stirred at rt for 1 h, then heated at reflux for 1 h under  $\text{N}_2$ . The solvent was removed and the residue dissolved in  $\text{CH}_3\text{CN}$  (50 mL). This solution was cooled to  $-15^\circ\text{C}$ .  $\text{TMSCH}_2\text{N}_2$  (2.0 M in hexane; 11 mL, 22 mmol) was added dropwise over 20 min. The reaction mixture was stirred at  $-15^\circ\text{C}$  for 1 h under  $\text{N}_2$ . A solution of HBr in HOAc (33% by mass; 4.25 mL) was added dropwise over 20 min, and the reaction mixture was stirred at  $-15^\circ\text{C}$  for an additional 20 min. The solvent was removed, and the residue dissolved in EtOAc, washed with water and brine, dried over  $\text{MgSO}_4$ , and concentrated to provide **13** (3.2 g, 39% yield over two steps), which was used in the next step without purification.  $^1\text{H}$  NMR (400 MHz,  $\text{CD}_3\text{OD}$ )  $\delta$  2.42 (s, 2H), 7.76–7.85 (m, 3H).  $m/z$  240, 242 (1:1)  $[\text{M} + \text{H}]^+$ .

**(S)-tert-Butyl 1-(4-(4-Cyano-3-fluorophenyl)-1H-imidazol-2-yl)-2-phenylethylcarbamate (14a).** To a solution of **13** (3.2 g, 13 mmol) and **7** (3.5 g, 13 mmol) in DMF (20 mL) was added  $\text{Cs}_2\text{CO}_3$  (2.6 g, 8 mmol). The reaction mixture was stirred at  $15^\circ\text{C}$  for 1 h under  $\text{N}_2$ . The mixture was diluted with 100 mL of EtOAc, washed with  $\text{H}_2\text{O}$ , brine, dried over  $\text{MgSO}_4$ , concentrated in vacuo, and purified by flash chromatography (240 g silica, 10–55% EtOAc in hexane) to yield (S)-2-(4-cyano-3-fluorophenyl)-2-oxoethyl 2-(tert-butoxycarbonylamino)-3-phenylpropanoate (**I-4**) (3.5 g, 63%).  $m/z$  425  $[\text{H} + \text{H}]^+$ . **I-4** was combined with  $\text{NH}_4\text{OAc}$  (12 g, 155 mmol) and suspended in xylenes (100 mL). The mixture was heated under  $\text{N}_2$  at  $150^\circ\text{C}$  for 2.5 h in a flask equipped with a Dean–Stark trap. The xylenes were removed in vacuo. The residue was dissolved in EtOAc, washed with  $\text{H}_2\text{O}$  and brine, dried over  $\text{MgSO}_4$ , concentrated in vacuo, and purified by flash chromatography (240 g silica, 15–70% EtOAc in hexane) to give **14a** (2.2 g, 41%).  $^1\text{H}$  NMR (400 MHz,  $\text{CDCl}_3$ )  $\delta$  1.39 (s, 9H), 3.30 (m, 2H), 4.86 (d,  $J = 6.6$  Hz, 1H), 5.32 (d,  $J = 7.5$  Hz, 1H), 7.14–7.24 (m, 6H), 7.53–7.61 (m, 3H).  $m/z$  407  $[\text{M} + \text{H}]^+$ .

**(S)-tert-Butyl 1-(5-Chloro-4-(4-cyano-3-fluorophenyl)-1H-imidazol-2-yl)-2-phenylethylcarbamate (14b).** To a solution of **14a** (2.2 g, 5.4 mmol) in  $\text{CH}_3\text{CN}$  (100 mL) was added NCS (0.80 g, 6.7 mmol). The reaction mixture was heated at reflux for 7 h under  $\text{N}_2$ . The solvent was removed in vacuo. The residue was dissolved in EtOAc, washed with  $\text{H}_2\text{O}$ , saturated aq  $\text{NaHCO}_3$ , and brine, dried over  $\text{MgSO}_4$ , and concentrated in vacuo to give **14b** (2.4 g, 99%). **14b** was used without purification.  $^1\text{H}$  NMR (400 MHz,  $\text{CDCl}_3$ )  $\delta$  1.27 (s, 9H), 3.23 (m, 2H), 4.89 (m, 1H), 5.46 (d,  $J = 7.0$  Hz, 1H), 7.07 (d,  $J = 6.2$  Hz, 2H), 7.25–7.26 (m, 5H), 7.54 (m, 1H).  $m/z$  441  $[\text{M} + \text{H}]^+$ .

**(S)-tert-Butyl 1-(4-(4-Cyano-3-fluorophenyl)-5-fluoro-1H-imidazol-2-yl)-2-phenylethylcarbamate (14c).** To a solution of **14a** (406 mg, 1 mmol) in DMF (10 mL) and  $\text{H}_2\text{O}$  (1 mL) was added Selecfluor (390 mg, 1.1 mmol). The reaction mixture was stirred at rt for 2 h, then diluted with  $\text{H}_2\text{O}$  and extracted with EtOAc. The combined organic extracts were washed with brine, dried over  $\text{Na}_2\text{SO}_4$ , filtered, and evaporated in vacuo. Purification by silica gel chromatography (40 g silica gel; EtOAc in hexanes) provided **14c** (113 mg, 27%).  $^1\text{H}$  NMR (400 MHz,  $\text{CDCl}_3$ )  $\delta$  1.37 (s, 9H), 3.10–3.30 (m, 2H), 4.81–4.89 (m, 1H), 5.42 (d,  $J = 7.1$  Hz, 1H), 6.90–7.00 (m, 2H), 7.08 (m, 2H), 7.21–7.27 (m, 3H), 7.45–7.52 (m, 1H), 11.01 (s, 1H).  $m/z$  425  $[\text{M} + \text{H}]^+$ .

**(S)-4-(2-(1-Amino-2-phenylethyl)-5-chloro-1H-imidazol-4-yl)-2-fluorobenzonitrile, Bis-trifluoroacetic Acid Salt (I-5).** **14b** (0.20 g, 0.45 mmol) was stirred with  $\text{CH}_2\text{Cl}_2$  (6 mL) and TFA (1.5 mL) under  $\text{N}_2$  for 0.5 h. The solvent and TFA were removed in vacuo to give **I-5** (0.26 g, 99%). **I-5** was used without purification.  $^1\text{H}$  NMR (400 MHz,  $\text{CD}_3\text{OD}$ )  $\delta$  3.33 (m, 2H), 4.56 (dd,  $J = 8.6$ , 6.4 Hz, 1H), 7.12 (d,  $J = 6.6$  Hz, 2H), 7.25–7.30 (m, 3H), 7.67 (m, 2H), 7.81 (m, 1H).  $m/z$  341  $[\text{M} + \text{H}]^+$ .

**tert-Butyl (trans-4-(((S)-1-(5-Chloro-4-(4-cyano-3-fluorophenyl)-1H-imidazol-2-yl)-2-phenylethyl)carbamoyl)-cyclohexyl)carbamate (I-6).** N-Boc-tranexamic acid (0.14 g, 0.54 mmol), BOP reagent (0.24 g, 0.54 mmol), and TEA (0.38 mL, 2.7 mmol) were combined in THF (10 mL). The reaction mixture was stirred at rt for 15 min under  $\text{N}_2$ , followed by the addition of **I-5** (0.26 g, 0.45 mmol). The resulting mixture was heated at  $75^\circ\text{C}$  for 15 min under  $\text{N}_2$ . The mixture was cooled to rt and the solvent removed in vacuo. The residue was dissolved in EtOAc. The solution was washed with  $\text{H}_2\text{O}$  and brine, dried over  $\text{MgSO}_4$ , concentrated in vacuo, and purified by flash chromatography (40 g silica, 10–100% EtOAc in hexane) to give intermediate **I-6** (0.21 g, 67%).  $^1\text{H}$  NMR (400 MHz,  $\text{CD}_3\text{OD}$ )  $\delta$  0.94 (m, 2H), 1.25–1.37 (m, 4H), 1.42 (s, 9H), 1.76–1.79 (m, 3H), 2.15 (m, 1H), 2.85 (m, 2H), 3.20–3.30 (m, 2H), 5.17 (m, 1H), 7.16–7.23 (m, 5H), 7.67–7.80 (m, 3H).  $m/z$  580  $[\text{M} + \text{H}]^+$ .

**trans-4-(Aminomethyl)-N-(((S)-1-(5-chloro-4-(4-cyano-3-fluorophenyl)-1H-imidazol-2-yl)-2-phenylethyl)cyclohexanecarboxamide, Bis-trifluoroacetic Acid Salt (15b).** **I-6** (0.21 g, 0.36 mmol) was stirred with  $\text{CH}_2\text{Cl}_2$  (8 mL) and TFA (2 mL) under  $\text{N}_2$  for 0.5 h. The solvent and TFA were removed in vacuo to give **15b** (0.25 g, >100%). **15b** was carried onto the next step without purification.  $m/z$  480  $[\text{M} + \text{H}]^+$ .

**trans-N-(((S)-1-(4-(3-Amino-1H-indazol-6-yl)-5-chloro-1H-imidazol-2-yl)-2-phenylethyl)-4-(aminomethyl)cyclohexanecarboxamide, Bis-trifluoroacetic Acid Salt (16b-2TFA).** **15b** (0.21 g, 0.36 mmol) and hydrazine monohydrate (0.69 mL) were combined in *n*-BuOH (8 mL). The reaction mixture was heated at  $120^\circ\text{C}$  under  $\text{N}_2$  for 1 h. The solvent was removed in vacuo and the product was purified by preparative HPLC to give **16b-2TFA** (0.14 g, 54%).  $^1\text{H}$  NMR (500 MHz,  $\text{CD}_3\text{OD}$ )  $\delta$  0.98–1.12 (m, 2H), 1.30–1.49 (m, 2H), 1.53–1.63 (m, 1H), 1.75 (d,  $J = 12$  Hz, 1H), 1.85 (d,  $J = 12$  Hz, 3H), 2.18–2.27 (m, 1H), 2.77 (d,  $J = 7.2$  Hz, 2H), 3.16 (dd,  $J = 13$ , 7.7 Hz, 1H), 3.25 (dd,  $J = 13$ , 7.7 Hz, 1H), 5.21 (t,  $J = 8.0$  Hz, 1H), 7.15–7.21 (m, 3H), 7.23–7.28 (m, 2H), 7.53 (dd,  $J = 8.5$ , 1.4 Hz, 1H), 7.71 (s, 1H), 7.98 (d,  $J = 8.8$  Hz, 1H). HRMS calcd for  $\text{C}_{26}\text{H}_{30}\text{ClN}_7\text{O}$  491.2200  $[\text{M} + \text{H}]^+$ , found 492.2283.

**Alternative Synthesis of Compound 16b Leading to the Bis-hydrochloric Acid Salt.** **tert-Butyl (trans-4-(((S)-1-(4-(3-Amino-1H-indazol-6-yl)-5-chloro-1H-imidazol-2-yl)-2-phenylethyl)carbamoyl)cyclohexyl)methylcarbamate (I-7).** To a slurry of **I-6** (4.4 g, 7.8 mmol) in *n*-BuOH (45 mL) was added hydrazine (14.5 mL, 462 mmol). The reaction mixture was heated to  $120^\circ\text{C}$  under Ar for 1 h. The solvent and excess hydrazine were removed in vacuo. The solids were washed with  $\text{Et}_2\text{O}$ , collected by filtration, and rinsed with additional  $\text{Et}_2\text{O}$  and then dried in vacuo to provide **I-7** (4.57 g, 99%). **I-7** was carried onto the next step without purification.  $m/z$  592  $[\text{M} + \text{H}]^+$ .

**trans-N-(((S)-1-(4-(3-Amino-1H-indazol-6-yl)-5-chloro-1H-imidazol-2-yl)-2-phenylethyl)-4-(aminomethyl)cyclohexanecarboxamide, Bis-hydrochloric Acid Salt (16b-2HCl).** Intermediate **I-7** (4.55 g, 7.7 mmol) was suspended in 4 N HCl in dioxane (45 mL). The reaction mixture was stirred at rt for 1.5 h. The mixture was dried in vacuo and the product purified by prep HPLC using buffer containing 0.05% HCl to afford **16b-2HCl** (1.88 g, 43%).  $^1\text{H}$  NMR (400 MHz,  $\text{CD}_3\text{OD}$ )  $\delta$  1.01–1.15 (m, 2H), 1.29–1.50 (m, 2H), 1.53–1.65 (m, 1H), 1.76–1.92 (m, 4H), 2.32 (tt,  $J = 12$ , 3.3 Hz, 1H), 2.78 (d,  $J = 7.0$  Hz, 2H), 3.35 (dd,  $J = 8.1$ , 2.9 Hz, 2H), 5.26 (t,  $J = 8.1$  Hz, 1H), 7.21–7.27 (m, 3H), 7.27–7.33 (m, 2H), 7.55 (dd,  $J = 8.8$ , 1.3 Hz, 1H), 7.80 (s, 1H), 8.10 (d,  $J = 8.8$  Hz, 1H).  $m/z$  492  $[\text{M} + \text{H}]^+$ .

**trans-N-(((S)-1-(4-(3-Amino-1H-indazol-6-yl)-1H-imidazol-2-yl)-2-phenylethyl)-4-(aminomethyl)cyclohexanecarboxamide, Bis-trifluoroacetic Acid Salt (16a).** Intermediate **14a** was converted to compound **16a** by using the methods used to convert **14b** to **16b**.

$^1\text{H}$  NMR (500 MHz,  $\text{CD}_3\text{OD}$ )  $\delta$  1.00–1.13 (m, 2H), 1.30–1.47 (m, 2H), 1.51–1.64 (m, 1H), 1.80 (d,  $J$  = 13 Hz, 1H), 1.86 (d,  $J$  = 12 Hz, 3H), 2.29 (tt,  $J$  = 12, 3.3 Hz, 1H), 2.77 (d,  $J$  = 7.2 Hz, 2H), 3.33 (dd,  $J$  = 8.8 Hz, 1 H, overlap with  $\text{CH}_3\text{OH}$ ), 3.38 (dd,  $J$  = 13, 8.2 Hz, 1H), 5.35 (t,  $J$  = 8.2 Hz, 1H), 7.20 (d,  $J$  = 7.2 Hz, 2H), 7.22–7.27 (m, 1H), 7.27–7.32 (m, 2H), 7.45 (d,  $J$  = 8.8 Hz, 1H), 7.72 (s, 1H), 7.91 (s, 1H), 7.98 (d,  $J$  = 8.8 Hz, 1H). HRMS calcd for  $\text{C}_{26}\text{H}_{31}\text{N}_7\text{O}$  458.2650  $[\text{M} + \text{H}]^+$ , found 458.2700.

**trans-N-((S)-1-(4-(3-Amino-1H-indazol-6-yl)-5-fluoro-1H-imidazol-2-yl)-2-phenylethyl)-4-(aminomethyl)cyclohexanecarboxamide, Bis-trifluoroacetic Acid Salt (16c).** Intermediate 14c was converted to compound 16c using the methods used to convert 14b to 16b.  $^1\text{H}$  NMR (400 MHz,  $\text{CD}_3\text{OD}$ )  $\delta$  7.94 (d,  $J$  = 8.2 Hz, 1H), 7.51 (s, 1H), 7.44 (d,  $J$  = 8.2 Hz, 1H), 7.28–7.21 (m, 2H), 7.21–7.14 (m, 3H), 5.18 (t,  $J$  = 8.0 Hz, 1H), 3.23 (dd,  $J$  = 13.7, 7.7 Hz, 1H), 3.14 (dd,  $J$  = 13.2, 8.2 Hz, 1H), 2.77 (d,  $J$  = 7.1 Hz, 2H), 2.28–2.17 (m, 1H), 1.91–1.79 (m, 3H), 1.79–1.70 (m, 1H), 1.65–1.51 (m, 1H), 1.50–1.29 (m, 2H), 1.13–0.98 (m, 2H).  $^{19}\text{F}$  NMR (471 MHz,  $\text{CD}_3\text{OD}$ )  $\delta$  –77.15 (s), –131.90 (s).  $m/z$  476  $[\text{M} + \text{H}]^+$ .

**(S)-2-(2-Phenyl-1-(5-phenyloxazol-2-yl)ethyl)isoindoline-1,3-dione (19).** To a solution of (S)-2-(1,3-dioxoisindolin-2-yl)-3-phenylpropanoic acid (17) (290 mg, 1 mmol) and 2-amino-1-phenylethanone (18) (171 mg, 1 mmol) in anhydrous pyridine (8 mL) was added BOP reagent (996 mg, 2.2 mmol). The reaction was stirred at rt for 16 h. The reaction was diluted with water and extracted with EtOAc. The combined organic extracts were washed with brine, dried over anhydrous  $\text{Na}_2\text{SO}_4$ , filtered, and evaporated to dryness in vacuo to yield 412 mg (100%) of crude (S)-2-(1,3-dioxoisindolin-2-yl)-N-(2-oxo-2-phenylethyl)-3-phenylpropanamide (I-8).  $m/z$  413  $[\text{M} + \text{H}]^+$ . To a solution of I-8 (412 mg, 1 mmol) in anhydrous DMF (1.7 mL) was added phosphorus oxychloride (460 mg, 3 mmol). The solution was heated to 90 °C for 20 min, cooled to rt, and poured onto ice. The resulting slurry was stirred for 30 min, then added to saturated aq  $\text{NaHCO}_3$  and extracted with EtOAc. The combined organic extracts were washed with  $\text{H}_2\text{O}$  and brine, dried over  $\text{Na}_2\text{SO}_4$ , filtered, and dried in vacuo. The product was purified by flash chromatography to yield 19 (160 mg, 41%).  $m/z$  395  $[\text{M} + \text{H}]^+$ .

**trans-4-(Aminomethyl)-N-((S)-2-phenyl-1-(5-phenyloxazol-2-yl)ethyl)cyclohexanecarboxamide, Bis-trifluoroacetic Acid Salt, Trifluoroacetic Acid Salt (20).** To a solution of compound 19 (160 mg, 0.4 mmol) in ethanol (10 mL) was added hydrazine (39 mg, 1.2 mmol). The reaction mixture was heated to reflux for 2 h. After cooling to rt, the solvent was removed in vacuo. The residue was dissolved in  $\text{CH}_2\text{Cl}_2$ , and insoluble solids were removed by filtration. The clear filtrate was concentrated to yield 95 mg (90%) of (S)-2-phenyl-1-(5-phenyloxazol-2-yl)ethanamine (I-9).  $m/z$  265  $[\text{M} + \text{H}]^+$ . I-9 (95 mg, 0.5 mmol) was converted to compound 20 (48 mg, 26%) using the procedures described for the conversion of compound I-2 to 11a.  $^1\text{H}$  NMR (500 MHz,  $\text{CD}_3\text{OD}$ )  $\delta$  1.04–1.10 (m, 2H), 1.29–1.42 (m, 2H), 1.56 (m, 1H), 1.75 (m, 1H), 1.83–1.86 (m, 3H), 2.22 (m, 1H), 2.77 (d,  $J$  = 7.2 Hz, 2H), 3.20 (m, 1H), 3.33 (m, 1H), 5.41 (m, 1H), 7.22–7.27 (m, 5H), 7.34 (t,  $J$  = 7.2 Hz, 1H), 7.42 (m, 3H), 7.63–7.65 (d,  $J$  = 8.2 Hz, 2H).  $m/z$  404  $[\text{M} + \text{H}]^+$ .

**(S)-tert-Butyl (2-Phenyl-1-(3-phenyl-1H-1,2,4-triazol-5-yl)ethyl)carbamate (21).** Compound 7 (265 mg, 1 mmol) and hydrazine (64 mg, 2 mmol) were combined using the conditions describe to convert I-2 to 10a and substituting hydrazine for N-Boc-tranexamic acid to give (S)-tert-butyl (1-hydrazinyl-1-oxo-3-phenylpropan-2-yl)carbamate (I-10) (279 mg, 100%).  $m/z$  280  $[\text{M} + \text{H}]^+$ . To a solution of I-10 (279 mg, 1.0 mmol) and  $\text{Et}_3\text{N}$  (161 mg, 1.6 mmol) in ACN (10 mL) was added ethyl benzimidate hydrochloride (278 mg, 1.5 mmol). The reaction was heated to reflux for 24 h, cooled to rt, and diluted with EtOAc. The mixture was washed with  $\text{H}_2\text{O}$  and brine, dried over  $\text{Na}_2\text{SO}_4$ , filtered, and evaporated to dryness in vacuo. The product was purified by preparative HPLC to yield 21 (154 mg, 42%).  $m/z$  365  $[\text{M} + \text{H}]^+$ .

**trans-4-(Aminomethyl)-N-((S)-2-phenyl-1-(3-phenyl-1H-1,2,4-triazol-5-yl)ethyl)-cyclohexanecarboxamide, Bis-trifluoroacetic Acid Salt (22).** Compound 21 (154 mg, 0.42 mmol) was converted to compound 22 (75 mg, 28%) using the methods described for the conversion of compound 9a to compound 11a.  $^1\text{H}$

NMR (400 MHz,  $\text{CD}_3\text{OD}$ )  $\delta$  1.02–1.06 (m, 2H), 1.29–1.42 (m, 2H), 1.56 (m, 1H), 1.75 (m, 1H), 1.83–1.86 (m, 3H), 2.21 (m, 1H), 2.77 (d,  $J$  = 7.0 Hz, 2H), 3.18–3.21 (m, 1H), 3.31 (m, 1H), 5.42 (t,  $J$  = 8.1 Hz, 1H), 7.22–7.26 (m, 5H), 7.51–7.52 (m, 3H), 7.96–7.98 (m, 2H).  $m/z$  404  $[\text{M} + \text{H}]^+$ .

**(S)-Benzyl (3,5-Dioxo-1,5-diphenylpentan-2-yl)carbamate (25).** To a solution of ethyl benzoylacetate (23) (2.88 g, 15 mmol) in EtOH (30 mL) was added 1 N aq NaOH (30 mL). The reaction mixture was stirred at rt for 72 h. The mixture was cooled to 0 °C and acidified with 1 N aq HCl. The EtOH was removed under reduced pressure. The aqueous layer was extracted with  $\text{CH}_2\text{Cl}_2$ . The combined organic extracts were washed with brine, dried over  $\text{Na}_2\text{SO}_4$ , filtered, and concentrated in vacuo to give 3-oxo-3-phenylpropanoic acid (I-11) (600 mg, 24%).  $m/z$  165  $[\text{M} + \text{H}]^+$ . To a solution of I-11 (600 mg, 3.65 mmol) in THF (20 mL) and  $\text{CH}_3\text{OH}$  (20 mL) was added magnesium ethoxide (417 mg, 3.65 mmol). The mixture was stirred at rt for 4 h. The solvents were removed in vacuo. The residue was dissolved in DMF (2 mL) and added to a mixture of N-Cbz-L-phenylalanine (24) (800 mg, 2.68 mmol) and 1,1'-carbonyldiimidazole (520 mg, 3.21 mmol) in DMF (4 mL), which had been stirred at rt for 2 h. The combined reaction mixture was stirred at rt for 16 h, diluted with EtOAc, washed with dilute aq HCl, water, and brine, dried over  $\text{Na}_2\text{SO}_4$ , filtered, and concentrated in vacuo. The product was isolated by prep HPLC to give 25 (140 mg, 13%).  $m/z$  402  $[\text{M} + \text{H}]^+$ .

**(S)-Benzyl (2-Phenyl-1-(3-phenyl-1H-pyrazol-5-yl)ethyl)carbamate (26).** To a solution of compound 25 (32 mg, 0.08 mmol) in EtOH (3 mL) was added hydrazine hydrate (3 mg, 0.09 mmol). The reaction mixture was heated at 60 °C for 3 h. EtOH was removed in vacuo to give compound 26 (32 mg, 100%).  $m/z$  398  $[\text{M} + \text{H}]^+$ .

**trans-4-(Aminomethyl)-N-((S)-2-phenyl-1-(3-phenyl-1H-pyrazol-5-yl)ethyl)cyclohexanecarboxamide, Bis-trifluoroacetic Acid Salt (27).** To a solution of compound 26 (32 mg, 0.06 mmol) in  $\text{CH}_3\text{OH}$  (3 mL) was added 10% Pd/C (5 mg). The reaction mixture was stirred under 1 atm of  $\text{H}_2$  at rt for 4 h. The catalyst was removed by filtration. The product was isolated by preparative HPLC to give (S)-2-phenyl-1-(3-phenyl-1H-pyrazol-5-yl)ethanamine (I-12) (12 mg, 76%).  $m/z$  262  $[\text{M} - \text{H}]^-$ . I-12 (12 mg, 0.046 mmol) was converted to compound 27 (11 mg, 46%) using the procedures described for the conversion of intermediate I-2 to 11a.  $^1\text{H}$  NMR (500 MHz,  $\text{CD}_3\text{OD}$ )  $\delta$  1.02–1.06 (m, 2H), 1.30–1.33 (m, 1H), 1.43–1.46 (m, 1H), 1.56 (m, 1H), 1.64 (m, 1H), 1.83 (m, 3H), 2.16–2.18 (m, 1H), 2.75 (d,  $J$  = 7.0 Hz, 2H), 3.08–3.10 (m, 1H), 3.27 (m, 1H), 5.35 (t,  $J$  = 8.1 Hz, 1H), 6.61 (s, 1H), 7.22 (m, 1H), 7.23 (m, 4H), 7.35–7.36 (t,  $J$  = 7.2 Hz, 1H), 7.41–7.44 (t,  $J$  = 7.7 Hz, 2H), 7.69–7.71 (d,  $J$  = 7.2 Hz, 2H).  $m/z$  403  $[\text{M} + \text{H}]^+$ .

**(S)-Benzyl (1-(5-Oxo-1-phenyl-4,5-dihydro-1H-1,2,4-triazol-3-yl)-2-phenylethyl)carbamate (29).** A solution of (S)-benzyl (1-cyano-2-phenylethyl)carbamate (28) (140 mg, 0.5 mmol) and sodium methoxide (13 mg, 0.24 mmol) in  $\text{CH}_3\text{OH}$  (4 mL) was stirred at 30 °C for 3 h. Acetic acid (14 mg, 0.24 mmol) was added followed by phenylhydrazine (108 mg, 1 mmol). The reaction mixture was stirred at rt for 18 h. The mixture was cooled to 0 °C, and solids were removed by filtration. The product was isolated by flash chromatography to give (S)-benzyl (1-imino-3-phenyl-1-(2-phenylhydrazinyl)propan-2-yl)carbamate (I-13) (55 mg, 28%).  $m/z$  389  $[\text{M} + \text{H}]^+$ . A solution of I-13 (55 mg, 0.14 mmol) and 1,1'-carbonyldiimidazole (68 mg, 0.42 mmol) in THF (6 mL) was heated to reflux for 48 h. The reaction was cooled to rt, diluted with  $\text{CH}_2\text{Cl}_2$ , washed with water and brine, dried over  $\text{Na}_2\text{SO}_4$ , filtered, and concentrated in vacuo to give 29 (38 mg, 66%). 29 was carried onto the next step without purification.  $m/z$  413  $[\text{M} - \text{H}]^-$ .

**trans-4-(Aminomethyl)-N-((S)-1-(5-oxo-1-phenyl-4,5-dihydro-1H-1,2,4-triazol-3-yl)-2-phenylethyl)cyclohexanecarboxamide, Trifluoroacetic Acid Salt (30).** Compound 29 (38 mg, 0.09 mmol) was converted to 30 (8 mg, 17%) by using the procedures described for the conversion of compound 26 to 27.  $^1\text{H}$  NMR (500 MHz,  $\text{CD}_3\text{OD}$ )  $\delta$  1.02–1.06 (m, 2H), 1.30–1.33 (m, 1H), 1.43–1.46 (m, 1H), 1.56 (m, 1H), 1.67 (m, 1H), 1.81–1.86 (m, 3H),



2.16–2.18 (m, 1H), 2.75 (d,  $J = 7.2$  Hz, 2H), 3.08–3.10 (m, 1H), 3.31 (m, 1H), 5.15–5.17 (m, 1H), 7.19–7.21 (m, 2H), 7.27–7.28 (m, 4H), 7.40–7.43 (t,  $J = 8.0$  Hz, 2H), 7.85–7.87 (d,  $J = 7.7$  Hz, 2H).  $m/z$  420.1  $[M + H]^+$ .

**(S)-Benzyl (2-Phenyl-1-(2-phenyl-1H-imidazol-4-yl)ethyl)-carbamate (32).** A solution of (S)-benzyl-(4-bromo-3-oxo-1-phenylbutan-2-yl) carbamate (**31**) (376 mg, 1.0 mmol) and sodium formate (68 mg, 1.0 mmol) in EtOH (15 mL) was heated to reflux for 14 h. Benzamidine (240 mg, 1.5 mmol) and sodium bicarbonate (400 mg, 4.7 mmol) were added to the mixture. The reaction mixture was heated to reflux for an additional 24 h. The mixture was cooled to rt and concentrated in vacuo. The residue was dissolved in EtOAc, washed with H<sub>2</sub>O and brine, dried over Na<sub>2</sub>SO<sub>4</sub>, filtered, and concentrated in vacuo. The product was isolated by flash chromatography to give **32** (33 mg, 8%).  $m/z$  398  $[M + H]^+$ .

**trans-4-(Aminomethyl)-N-((S)-2-phenyl-1-(2-phenyl-1H-imidazol-4-yl)ethyl)cyclohexanecarboxamide, Bis-trifluoroacetic Acid Salt (33).** Compound **32** (33 mg, 0.08 mmol) was converted to compound **33** (5 mg, 12%) using the procedures described for the conversion of compound **26** to **27**. <sup>1</sup>H NMR (400 MHz, CD<sub>3</sub>OD)  $\delta$  1.02–1.06 (m, 2H), 1.30–1.33 (m, 1H), 1.43–1.46 (m, 1H), 1.56 (m, 1H), 1.67 (m, 1H), 1.83 (m, 3H), 2.16–2.18 (m, 1H), 2.75 (d,  $J = 7.0$  Hz, 2H), 3.08–3.10 (m, 1H), 3.31 (m, 1H), 5.34–5.36 (m, 1H), 7.22–7.29 (m, 5H), 7.51 (s, 1H), 7.62–7.68 (m, 3H), 7.87–7.89 (m, 2H).  $m/z$  403  $[M + H]^+$ .

## ■ ASSOCIATED CONTENT

### ■ Supporting Information

Crystallographic data and refinement statistics. This material is available free of charge via the Internet at <http://pubs.acs.org>.

## ■ AUTHOR INFORMATION

### Corresponding Author

\*Phone: +1 609 818 4958. Fax: +1 609 818 3560. E-mail: [jon.hangeland@bms.com](mailto:jon.hangeland@bms.com).

### Notes

The authors declare no competing financial interest.

## ■ ACKNOWLEDGMENTS

Use of the IMCA-CAT beamline 17-ID at the Advanced Photon Source was supported by the companies of the Industrial Macromolecular Crystallography Association through a contract with the Illinois Institute of Technology. Use of the Advanced Photon Source was supported by the U.S. Department of Energy, Office of Science, Office of Basic Energy Sciences, under Contract DE-AC02-06CH11357. We thank Dr. Steven Sheriff for final refinement of the X-ray crystal structures for the FXIa/11h and FXIa/16b complexes and for depositing the coordinates and X-ray data in the Protein Data Bank, Dr. William R. Ewing and Dr. R. Michael Lawrence for assistance editing the manuscript, and Jergen Bauman, Dr. Eileen Bird, Dr. Baomin Xin, and Gang Luo for obtaining the rabbit pharmacokinetic data.

## ■ ABBREVIATIONS USED

aPTT, activated partial thromboplastin time; AV, arterovenous; ECAT, electrically mediated carotid arterial thrombosis; FVIIa, activated coagulation factor VII; FVIIIa, activated coagulation factor VIII; FIXa, activated coagulation factor IX; FXa, activated coagulation factor X; FXIa, activated coagulation factor XI; FXIIa, activated coagulation factor XII; IPTG, isopropyl  $\beta$ -D-1-thiogalactopyranoside; PK, plasma kallikrein; PT, prothrombin time; TAFI, thrombin-activatable fibrinolysis inhibitor; TF, tissue factor; TT, thrombin time; VT, venous thrombosis

## ■ REFERENCES

- (1) (a) Jackson, S. P. *Nat. Med.* **2011**, *17*, 1423–1436. (b) Global Status Report on Noncommunicable Diseases 2010. WHO Press: Geneva, Switzerland, 2011. (c) WHO Fact Sheet No. 310. World Health Organization: Geneva, Switzerland, June 2011.
- (2) (a) McFarlane, R. An enzyme cascade in the blood clotting mechanism, and its function as a biochemical amplifier. *Nature* **1964**, *202*, 498–499. (b) Davie, E. W.; Ratnoff, O. Waterfall sequence for intrinsic clotting. *Science* **1964**, *145*, 1310–1313. (c) Davie, E. W.; Fujikawa, K.; Kisiel, W. The coagulation cascade: initiation, maintenance and regulation. *Biochemistry* **1991**, *30*, 10363–10370. (d) Gailani, D.; Broze, G. Factor XI activation in a revised model of blood coagulation. *Science* **1991**, *253*, 909–912. (e) Müller, F.; Mutch, N. J.; Schenk, W. A.; Smith, S. A.; Esterl, L.; Spronk, H. M.; Schmidbauer, S.; Gahl, W. A.; Morrissey, J. H.; Renné, T. Platelet polyphosphates are proinflammatory and procoagulant mediators in vivo. *Cell* **2009**, *139*, 1143–1156. (f) Chatterjee, K.; Guo, Z.; Vogler, E. A.; Siedlecki, C. A. Contributions of contact activation pathways of coagulation factor XII in plasma. *J. Biomed. Mater. Res.* **2009**, *90A*, 27–34.
- (3) (a) Asakai, R.; Chung, D.; Davie, E.; Seligsohn, U. Factor XI deficiency in Ashkenazi Jews in Israel. *N. Engl. J. Med.* **1991**, *325*, 153–158. (b) Gailani, D.; Broze, G. J. Factor XI and the Contact System. In *The Metabolic and Molecular Basis of Inherited Disease*, 8th ed.; Scriver, C. R., Beaudet, A. L., Sly, W. S., Valle, D., Childs, B., Kinzler, K. W., Vogelstein, B., Eds.; McGraw-Hill: New York, 2001; p 4433. (c) Gailani, D.; Renné, T. The intrinsic pathway for coagulation: A target for treating thromboembolic disease? *J. Thromb. Haemostasis* **2007**, *5*, 1106–1112. (d) Schumacher, W.; Luettggen, J.; Quan, M. L.; Seiffert, D. Inhibition of factor XIa as a new approach to anticoagulant. *Arterioscler., Thromb., Vasc. Biol.* **2010**, *30*, 388–392.
- (4) Bolton-Maggs, P. H.; Patterson, D. A.; Wensley, R. T.; Tuddenham, E. G. Definition of the bleeding tendency in factor XI-deficient kindreds—a clinical and laboratory study. *Thromb. Haemostasis* **1995**, *73*, 194–202.
- (5) Lozier, J. N.; Kessler, C. M. Clinical Aspects and Therapy of Hemophilia. In *Hematology: Basic Principles and Practice*, 4th ed.; Hoffman, R., Benz, E., Shattil, S., Furie, B., Cohen, H., Silberstein, L., McGlave, P., Eds.; Churchill Livingstone: New York, 2005; p 2047.
- (6) Wang, X.; Smith, P. L.; Hsu, M.-Y.; Gailani, D.; Schumacher, W. A.; Ogletree, M. L.; Seiffert, D. A. Effects of factor XI deficiency on ferric chloride-induced vena cava thrombosis in mice. *J. Thromb. Haemostasis* **2006**, *4*, 1982–1988.
- (7) (a) Yang, D. T.; Flanders, M. M.; Kim, H.; Rodgers, G. M. Elevated factor XIa activity levels are associated with an increased odds ratio for cerebrovascular events. *Am. J. Clin. Pathol.* **2006**, *126*, 411–415. (b) Butenas, S.; Undas, A.; Gissel, M. T.; Szuldrzynski, K.; Zmudka, K.; Mann, K. G. Factor XIa and tissue factor activity in patients with coronary artery disease. *Thromb. Haemostasis* **2008**, *99*, 142–149.
- (8) Salomon, O.; Steinberg, D. M.; Koren-Morag, N.; Tanne, D.; Seligsohn, U. Reduced incidence of ischemic stroke in patients with severe factor XI deficiency. *Blood* **2008**, *111*, 4113–4117.
- (9) (a) Lin, J.; Deng, H.; Jin, L.; Pandey, P.; Quinn, J.; Cantin, S.; Rynkiewicz, M. J.; Gorga, J. C.; Bibbins, F.; Celatka, C. A.; Nagafuji, P.; Bannister, T. D.; Meyers, H. V.; Babine, R. E.; Hayward, N. J.; Weaver, D.; Benjamin, H.; Stassen, F.; Abdel-Meguid, S. S.; Strickler, J. E. Design, Synthesis, and Biological Evaluation of Peptidomimetic Inhibitors of Factor XIa as Novel Anticoagulants. *J. Med. Chem.* **2006**, *49*, 7781–7791. (b) Deng, H.; Bannister, T. D.; Jin, L.; Babine, R. E.; Quinn, J.; Nagafuji, P.; Celatka, C. A.; Lin, J.; Lazarova, T. I.; Rynkiewicz, M. J.; Bibbins, F.; Pandey, P.; Gotga, J.; Meyers, H. V.; Abdel-Meguid, S. S.; Strickler, J. E. Synthesis, SAR exploration, and X-ray crystal structures of factor XIa inhibitors containing an  $\alpha$ -ketothiazole arginine. *Bioorg. Med. Chem. Lett.* **2006**, *16*, 3049–3054.
- (10) (a) Schumacher, W. A.; Seiler, S. E.; Steinbacher, T. E.; Stewart, A. B.; Bostwick, J. B.; Hartl, K. S.; Liu, E. C.; Ogletree, M. L. Antithrombotic and hemostatic effects of a small molecule factor XIa inhibitor in rats. *Eur. J. Pharmacol.* **2007**, *570*, 167–174. (b) Wong, P.

- C.; Crain, E. J.; Watson, C. A.; Schumacher, W. A. A small-molecule factor XIa inhibitor produces antithrombotic efficacy with minimal bleeding time prolongation in rabbits. *J. Thromb. Thrombolysis* **2011**, *32*, 129–137.
- (11) Sutton, J. C.; Bolton, S. A.; Hartl, K. S.; Huang, M.-H.; Jacobs, G.; Meng, W.; Ogletree, M. L.; Pi, Z.; Schumacher, W. A.; Seiler, S. M.; Slusarchyk, W. A.; Treuner, U.; Zhaller, R.; Zhao, G.; Basicchi, G. S. Synthesis and SAR of 4-carboxy-2-azetidinone mechanism-based tryptase inhibitors. *Bioorg. Med. Chem. Lett.* **2002**, *12*, 3229–3233.
- (12) Quan, M. L.; Wong, P. C.; Wang, C.; Woerner, F.; Smallheer, J. M.; Barbera, F. A.; Bozarth, J. M.; Brown, R. L.; Harpel, M. R.; Luetgen, J. M.; Morin, P. E.; Peterson, T.; Ramamurthy, V.; Rendina, A. R.; Rossi, K. A.; Watson, C. A.; Wei, A.; Zhang, G.; Seiffert, D.; Wexler, R. R. *J. Med. Chem.* **2014**, *57*, 955–969.
- (13) Wong, P. C.; Quan, M. L.; Watson, C.; Crain, E.; Wexler, R. R.; Seiffert, D. Potent Antithrombotic Effect of a Small-Molecule, Reversible and Direct Inhibitor of Factor XIa with Minimum Bleeding Time Effect in Rabbit Models of Arterial Thrombosis and Hemostasis. Presented at the American Heart Association Scientific Sessions, November 2013; APS.709.03, Poster 7050.
- (14) Buchanan, M. S.; Carroll, A. R.; Wessling, D.; Jobling, M.; Avery, V. M.; Davis, R. A.; Feng, Y.; Zue, Y.; Fex, T.; Deinum, J.; Hooper, J. N. A.; Quinn, R. J. Clavatadine A, a natural product with selective recognition and irreversible inhibition of factor XIa. *J. Med. Chem.* **2008**, *51*, 3583–3587.
- (15) Lazarova, T. I.; Jin, L.; Rynkiewicz, M.; Gorga, J. C.; Bibbins, F.; Meyers, H. V.; Babine, R.; Strickler, J. Synthesis and in vitro biological evaluation of aryl boronic acids as potential inhibitors of factor XIa. *Bioorg. Med. Chem. Lett.* **2006**, *16*, 5022–5027.
- (16) Smallheer, J. M.; Wang, S.; Rossi, K. A.; Rendina, A.; Morin, P. E.; Wei, A.; Zhang, G.; Wong, P. C.; Seiffert, D.; Wexler, R. R.; Quan, M. L. *Abstracts of Papers*, 245th National Meeting of the American Chemical Society, New Orleans, LA, U.S., April 7–11, 2013; American Chemical Society: Washington, DC, 2013; MEDI-415.
- (17) (a) Sinha, D.; Badellina, K. O.; Marcinkiewicz, M.; Walsh, P. N. Allosteric modification of factor XIa functional activity upon binding to polyanions. *Biochemistry* **2004**, *43*, 7593–7600. (b) Argade, M. D.; Mehta, A. Y.; Sarkar, A.; Desai, U. R. Allosteric inhibition of human factor XIa: discovery of monosulfated benzofurans as a class of promising inhibitors. *J. Med. Chem.* **2014**, *57*, 3559–3569. (c) Al-Horani, R. A.; Desai, U. R. Designing allosteric inhibitors of factor XIa. Lessons from the interactions of sulfated pentagalloyl-glucopyranosides. *J. Med. Chem.* **2014**, *57*, 4805–4818. (d) Al-Horani, R. A.; Ponnusamy, P.; Mehta, A. Y.; Gailani, D.; Desai, U. R. Sulfated pentagalloylglucoside is a potent, allosteric, and selective inhibitor of factor XIa. *J. Med. Chem.* **2013**, *56*, 867–878. (e) Karuturi, R.; Al-Horani, R. A.; Mehta, S. C.; Gailani, D.; Desai, U. R. Discovery of allosteric modulators of factor XIa by targeting the hydrophobic domains adjacent to its heparin-binding site. *J. Med. Chem.* **2013**, *56*, 2415–2428. (f) Ma, D.; Mizurini, D. M.; Assumpcao, T. C. F.; Li, Y.; Qi, Y.; Kotsyfakis, M.; Ribeiro, J. M. C.; Monteiro, R. Q.; Francischetti, I. M. B. Desmolaris, a novel factor XIa anticoagulant from the salivary gland of the vampire bat (*Desmodus rotundus*) inhibits inflammation and thrombosis in vivo. *Blood* **2013**, *122*, 4094–4106.
- (18) (a) Wong, P. C.; Quan, M. L.; Crain, E. J.; Watson, C. A.; Wexler, R. R.; Knabb, R. M. Nonpeptide factor Xa inhibitors: studies with SF303 and SK549, a new class of potent antithrombotics. *J. Pharmacol. Exp. Ther.* **2000**, *292*, 351–357. (b) Wong, P. C.; Crain, E. J.; Knabb, R. M.; Meade, R. P.; Quan, M. L.; Watson, C. A.; Wexler, R. R.; Wright, M. R.; Slee, A. M. Nonpeptide factor Xa inhibitors II. Antithrombotic evaluation in a rabbit model of electrically induced carotid artery thrombosis. *J. Pharmacol. Exp. Ther.* **2000**, *295*, 212–218. (c) Wong, P. C.; Crain, E. J.; Watson, C. A.; Zaspel, A. M.; Wright, M. R.; Lam, P. Y.; Pinto, D. J. P.; Wexler, R. R.; Knabb, R. M. Nonpeptide factor Xa inhibitors III. Effects of DPC423, an orally-active pyrazole antithrombotic agent, on arterial thrombosis in rabbits. *J. Pharmacol. Exp. Ther.* **2000**, *303*, 993–1000. (d) Himber, J.; Kirchhofer, D.; Riederer, M.; Tschopp, T. B.; Steiner, B.; Roux, S. P. Dissociation of antithrombotic effect and bleeding time prolongation in rabbits by inhibiting tissue factor function. *Thromb. Haemostasis* **1997**, *78*, 1142–1149.
- (19) Bird, J. E.; Smith, P. L.; Wang, X.; Schumacher, W. A.; Barbera, F.; Revelli, J.-P.; Seiffert, D. Effects of plasma kallikrein deficiency on haemostasis and thrombosis in mice: murine ortholog of the Fletcher trait. *Thromb. Haemostasis* **2012**, *107*, 1141–1150.
- (20) Contour-Galcerá, M.-O.; Poitout, L.; Moinet, C.; Morgan, B.; Gordon, T.; Roubert, P.; Thurié, C. Synthesis of substituted imidazopyrazines as ligands for the human somatostatin receptor subtype 5. *Bioorg. Med. Chem. Lett.* **2001**, *11*, 741–745.
- (21) Otwinowski, Z.; Minor, W. *Macromolecular Crystallography. Part A*; Carter, C. W., Sweet, R. M., Eds.; Methods in Enzymology, Vol. 276; Academic Press, Inc., San Diego, CA, 1997; pp 307–326.
- (22) Blanc, E.; Roversi, P.; Vonnheim, C.; Flensburg, C.; Lea, S. M.; Bricogne, G. Refinement of severely incomplete structures with maximum likelihood in BUSTER/TNT. *Acta Crystallogr., Sect. D: Biol. Crystallogr.* **2004**, *60*, 2210–2221.
- (23) Emsley, P.; Lokhamp, B.; Scott, W. G.; Cowtan, K. Features and Development of Coot. *Acta Crystallogr., Sect. D: Biol. Crystallogr.* **2010**, *66*, 486–501.
- (24) Laskowski, R. A.; MacArthur, M. W.; Moss, D. S.; Thornton, J. M. PROCHECK: a program to check the stereochemical quality of protein structures. *J. Appl. Crystallogr.* **1993**, *26*, 283–291.